https://doi.org/10.5194/hess-2024-55
Preprint. Discussion started: 13 March 2024

Hydrology and Earth System Sciences
Discussions

How much water vapour does the Tibetan Plateau release into the atmosphere?

Chaolei Zheng[1], Li Jia[1], Guangcheng Hu [1], Massimo Menenti[1, 2], Joris Timmermans[2]

[1] State Key Laboratory of Remote Sensing Science, Aerospace Information Research Institute, Chinese Academy of Sciences, Beijing 100101, China
[2] Faculty of Civil Engineering and Geosciences, Delft University of Technology, Delft, the Netherlands

Correspondence to: Chaolei Zheng (zhengcl@aircas.ac.cn)

Abstract. Evapotranspiration (ET) is critical for understanding the earth climate system and the complex heat/water exchange mechanisms between the land surface and the atmosphere in the high-altitude Tibetan Plateau (TP) region. However, the performance of ET products over TP has not been adequately assessed, and there is still significant uncertainty regarding the amount of water vapour released by the TP into the atmosphere, as well as its variation. In this study, we evaluated 22 ET products over TP by validating with the in-situ observations and basin-scale water balance estimations. This study also inter-compared their spatiotemporal variations and components to clarify the ET magnitude and variability in TP. The results showed that the remote sensing high-resolution global ET data from ETMonitor and PMLV2 demonstrated high accuracy comparable to the regional MOD16STM ET product, with overall better accuracy than other global ET data with fine spatial resolution (~1km), when comparing with in-situ observation. Their accuracy was also presented when compared with the water balance-based ET at basin scale, which further indicated the overall accuracy of GLEAM and TerraClimate for the coarse-resolution ET products. Different products showed different spatiotemporal variation patterns, with large discrepancy occurring in the middle to western TP. The multiple-year averaged ET over TP by these products was found to have an average value (standard deviation) of 350.34 (42.46) mm/yr. The different components (plant transpiration, soil evaporation, canopy rainfall interception evaporation, open water evaporation, and snow/ice sublimation) available from some products were also compared, and the separate contribution of these components varied substantially even in cases in which total ET agrees by different products. The response of annual ET to total precipitation, net radiation and leaf area index was explored to present their governing effect on ET, and the results indicated that precipitation effect mostly in the middle and northern TP and net radiation play significant role in the eastern TP.

1 Introduction

The TP is also known as the "Water Tower of Asia" as it is the source of 10 major river basins. Significant changes have occurred in the natural and social environments of TP over the past 50 years (e.g., temperatures warming twice as much as the global average over the same period), providing a significant uncertainty of further environmental change (Immerzeel et al., 2020; Yang et al., 2014; Chen et al., 2015). Observations have shown significant changes in the environment, such as increased

https://doi.org/10.5194/hess-2024-55
Preprint. Discussion started: 13 March 2024

Hydrology and Earth System Sciences
Discussions

precipitation, decreased wind speed and snow days, increasing at-surface solar irradiance, thawing of permafrost, melting of glaciers and snow, and greening of vegetation (Yao et al., 2012; Yang et al., 2014; Kuang and Jiao et al., 2016; Bibi et al., 2018; Z. Wang et al., 2018). These changes have had significant impacts on human living environment, as well as economic and social development (Wei et al., 2022; Yang et al., 2022). TP can also affect the atmospheric circulation by altering the release of sensible and latent heat, which has a significant impact on the climate in China, Asia, and globally (Wu et al., 2016).

Studying evapotranspiration (ET) over the Tibetan Plateau (TP) is critical for understanding the earth climate system and the complex heat/water exchange mechanisms (Shen et al., 2015; Yang et al., 2023). ET plays a crucial role in linking the water and energy cycles in the hydrosphere, atmosphere, soil and biosphere. It is important as a covariate of the water and heat fluxes in the soil-vegetation-atmosphere system in the TP and as an indicator of climate and land surface changes (Sun et al., 2023; Yang et al. 2023; Zhang et al., 2010). It is expected that TP is experiencing faster water phase transformation, with more solid water becoming liquid water by melting glacier/snow and more liquid water vaporized through ET (Z. Li et al., 2019; Yao et al., 2019). Estimating ET at a large scale around the TP has always been challenging due to the area's high heterogeneity and the harsh conditions. The TP is rich in land cover types, including grasslands, deserts, lakes, forests, glaciers, snow, and so on. The dynamics and thermodynamics of the subsurface vary greatly among different climate types, making it a great challenge to conduct large-scale studies of ET processes on TP and explore the governing mechanism and feedback effect on the climate system and hydrological processes. In addition, the harsh natural conditions and ecological environment of the plateau make ground-based observations difficult, and the high cost of instrumentation and routine maintenance have resulted in a scarcity of evapotranspiration stations on the TP and a relatively short time series of observations (Ma et al., 2020).

ET estimation from land surface models (LSMs) and climate reanalysis has been widely adopted, however generally with coarse spatial resolutions (e.g., 0.25°) and suffers from large accumulated errors due to many factors, e.g., the uncertainty of driven forces and model parametrization, surface heterogeneity, etc. (Chen et al., 2019; Khan et al., 2020; X. Li et al., 2019). In contrast, ET estimation based on satellite remote sensing observations that allow for high-resolutions estimation has obvious advantages, especially in the spatially heterogeneous regions of TP (Ma et al. 2006; Jia et al. 2018; Zheng et al. 2016). During the last decades, the remote sensing-based ET datasets have been improved significantly, and several regional and global, high quality ET datasets have been produced (e.g., Chen et al., 2021; Martens et al., 2017; Elnashar et al., 2021; Jia et al., 2018). For example, the validation results based on the global flux network show that the PMLV2 and ETMonitor global ET products have good accuracy (with RMSE<1mm/d) (Zhang et al., 2019b; Zheng and Jia, 2020). These improved ET datasets also have many advantages, e.g., the ability to distinguish different components (vegetation transpiration, soil evaporation, and canopy rainfall interception loss), higher spatial resolution (e.g., 1-km), better behavior in the heterogeneous land surface, but their application to the Tibetan Plateau deserves further attention. However, previous studies also found significant differences between different products, such as divergent magnitudes of the annual mean ET in TP from 294 mm/yr (Wang et al., 2020) to 543 mm/yr (Zhang et al., 2018), and varying trends of ET depending on the adopted datasets and study periods (Ma and Zhang, 2022; Wang et al. 2022). Inter-comparing different ET products certainly contribute to understand the ET process in

https://doi.org/10.5194/hess-2024-55
Preprint. Discussion started: 13 March 2024


Hydrology and Earth System Sciences
Discussions

TP, as well the ET magnitude and variations, which also there is a need to strengthen research on TP as a whole region and improve the understanding of the changing patterns of the Tibetan Plateau's water cycle and eco-hydrological processes (W. Wang et al., 2018).

The performance of ET product is related to both the adopted algorithms and the driving variables of the model (Mueller et al., 2013; Wang et al., 2022). Specifically, the contributions of different processes (e.g., plant transpiration, soil evaporation, water evaporation from canopy intercepted rainfall and open water body) to total water flux of individual products vary due to the theoretical and technological differences of different models (Chen et al., 2021; Cui et al., 2020; Hu et al., 2009; Zhu et al. 2021, Ma and Zhang, 2022; Miralles et al., 2020). The global ET datasets based on satellite remote sensing were criticized for the lack of adaption to specificity for the special environment of TP and the uncertainty inherited from the input global meteorological reanalysis data, which may lead to a large uncertainty when directly applying the global ET in TP (Zou, 2020; Song et al. al., 2017; Chang et al., 2018; Xue et al., 2013). These validations were generally based on either *in-situ* measurement by the eddy covariance system or the basin-scale ET estimated by water balance method, which represent the surface net water flux that integrates different processes (e.g., plant transpiration for the dense vegetation regions, snow sublimation for the dry snow cover periods for the eddy covariance system observations, even condensation when negative latent heat flux occurs), while these ET products mainly focus on the ET (positive upward latent heat flux), which attributes to the validation uncertainty. In the evaluation of satellite remote sensing products against ground-based measurements and the inter-comparison between products, these specificities however are generally not included.

The following questions should be addressed: 1) How accurate are these improved ET products, and how do different products agree to capture the ET magnitude and variability in the TP? 2) How much water is vaporized in TP and which processes, e.g., plant transpiration, soil evaporation, snow/ice sublimation, play a significant role? 3) How do different products respond to environmental factors, e.g., precipitation? Answering these questions would reveal strengths and weaknesses of different ET products and address the knowledge gaps on relevant processes over TP, which is fundamental for different scientific and practical purposes.

The aim of this paper is to clarify the ET magnitude and variability in TP by assessing and inter-comparing the accuracy and spatiotemporal variations of ET over TP from common available gridded products. Specifically, the main objectives include 1) to estimate the absolute uncertainties of individual ET products; 2) to evaluate the spatiotemporal variations and components of ET between different ET products; 3) to assess the response of ET in TP to the environmental factors. To estimate the absolute uncertainty of the different ET data products, we will use a validation approach using data from flux towers and water balance estimates. Afterwards, to evaluate the spatiotemporal variations and partitioning, we will intercompare the spatial variation of the different ET products using both multiple-year averaged annual ET and the seasonal variation of ET. Finally, we will assess the response of ET in TP to precipitation, net surface radiation and leaf area index based on the Pearson correlation analysis.

https://doi.org/10.5194/hess-2024-55
Preprint. Discussion started: 13 March 2024

Hydrology and Earth System Sciences
Discussions

2 Methodology and Data

2.1 Study region

The Tibetan Plateau (25-40°N, 70-105°E) is the highest elevated region in the world, covering an area of approximately 3.0 million km^2 with most region above 2,500 meters in altitude (Figure 1). It has complex climatic regimes, including humid, semi-humid, monsoon, semi-arid, arid, and hyper-arid climates. Influenced by multiple water vapor sources through atmospheric circulation and alpine terrain, its precipitation presents spatial variability with the average annual precipitation gradually increasing from less than 50 mm/yr in the northwest to more than 1000 mm/yr in the southeast, and most of the precipitation concentrated in summer (Jiang et al., 2023). The TP is also known for its extensive snow and glacier coverage, with a total glacier area of approximately 50,000 km^2 (Yao et al., 2007) and 77% area above 6000m above sea level covered by snow (Chu et al. 2023). The land cover types are mainly forest, grassland, bare soil, glaciers and snow (Supplementary Figure S1). The dense river network on TP, which includes the headwaters of five major Asian rivers, is primarily formed by precipitation and the meltwater from glaciers and snowpack.

The TP region comprises 12 subregions: Hexi, Tarim, Qaidam, Upper Amu Darya, Inner TP, Upper Yellow, Upper Yangtze, Upper Salween, Upper Mekong, Upper Brahmaputra, Upper Ganges, and Upper Indus (Figure 1). The first five subregions, Hexi, Tarim, Qaidam, Amu Darya, and Inner TP, are located in the northern, western, and central parts of TP and experience relatively low precipitation. The remaining watersheds receive high precipitation due to the monsoons originating from the Arabian Sea, the South China Sea, and the Western Pacific, and extreme high annual precipitation (>1000mm/yr) are found in Upper Salween, Upper Brahmaputra, and Upper Ganges.

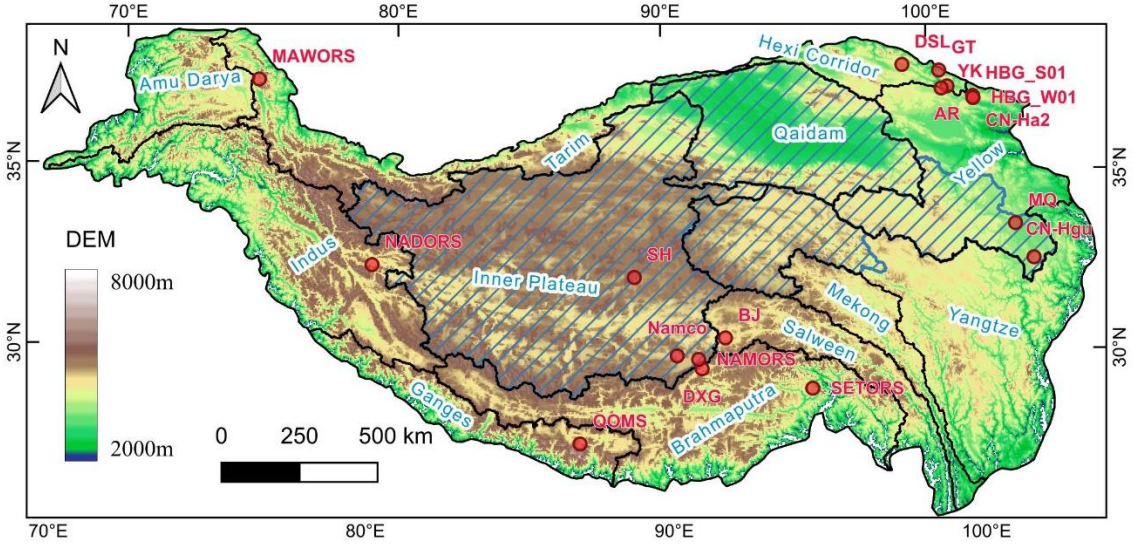

Figure 1: Location of the selected ground flux tower observation sites and major river basins in the Tibetan Plateau, with elevation shown as background.

https://doi.org/10.5194/hess-2024-55
Preprint. Discussion started: 13 March 2024

Hydrology and Earth System Sciences
Discussions

2.2 Data sources

2.2.1 Flux tower data

To validate ET at high spatial resolution (≤1km), measurements of near-surface turbulent fluxes by the eddy-covariance method at 18 flux towers were collected. Figure 1 presents the spatial distribution of these sites, and the details are provided in Table 1. The quality of flux observation data at each site was evaluated after data screening, and only reliable observations were selected following the methodology described by Zheng et al. (2022). These the sites, where gap-filled daily or monthly ET data with reliable quality were already available (DXG, HBG-S01, HBG-W01, CN-HaM, CN-Hgu, SH, Maqu), were directly adopted without further modification. For sites that provide half-hourly or hourly data, the observed latent heat flux data were gap-filled after energy closure correction, and this includes six sites (BJ, NADORS, SETORS, QOMS, NAMORS, MAWORS) from the Tibetan Observation and Research Platform (Ma et al., 2020; 2008), four sites from the Heihe Integrated Observatory Network (Liu et al., 2018; Li et al., 2009), and our own site at Namco. The Bowen ratio energy balance correction method preserves the Bowen ratio by attributing the residual term of the energy balance to the latent heat flux and sensible heat flux (Twine et al., 2000; Foken, 2008; Chen et al., 2014). The corrected half-hourly or hourly LE data was then averaged to obtaine daily ET values, and only the days with more than 80% of the hourly flux were retained as valid observations. The missing daily ET values were further filled using the constant reference evapotranspiration fraction method (Jiang et al., 2022). The monthly ET was finally calculated by accumulating the daily ET values, and those months with less than 50% valid daily ET values were excluded.

Table 1: List of ground flux tower observation sites.

Site Code	Site Name	Latitude/Longitude	Elevation	Land Cover	Periods	Sources /reference
MAWORS	TORP MAWORS	38.41 ºN, 75.05 ºE	3668	Desert steppe	2012-2016	Ma et al., 2020
NADORS	TORP NADORS	33.39 ºN, 79.70 ºE	4270	Desert steppe	2010–2018	Ma et al., 2020
NAMORS	TORP NAMORS	30.77 ºN, 90.96 ºE	4730	Alpine steppe	2008–2018	Ma et al., 2020
QOMS	TORP QOMS	28.36 ºN, 86.95 ºE	4298	Desert steppe	2007–2018	Ma et al., 2020
SETORS	TORP SETORS	29.77 ºN, 94.74 ºE	3327	Alpine meadow	2007–2018	Ma et al., 2020
BJ	TORP BJ	31.37 ºN, 91.90 ºE	4509	Sparse alpine meadow	2010–2016	Ma et al., 2020
SH	TORP Shuanghu	33.21 ºN, 88.83 ºE	4947	Alpine steppe	2013–2018	Ma et al., 2015
ARS	HiWATER A'rou	38.05 ºN, 100.46 ºE	3033	Dense alpine meadow	2008–2018	Liu et al., 2018
DSL	HiWATER Dashalong	38.84 ºN, 98.94 ºE	3739	Alpine meadow	2013-2018	Liu et al., 2018
YK	HiWATER Yakou	38.01 ºN, 100.24 ºE	4148	Alpine steppe	2014-2018	Liu et al., 2018
GT	HiWATER Guantan	38.53 ºN, 100.25 ºE	2835	Needleleaf forest	2009-2011	Li et al., 2009
DXG	ChinaFLUX Dangxiong	30.49 ºN, 91.07 ºE	4333	Alpine meadow	2004–2010	Yu et al., 2006

https://doi.org/10.5194/hess-2024-55
Preprint. Discussion started: 13 March 2024

Hydrology and Earth System Sciences Discussions

HBG-S01	ChinaFLUX Haibei grassland	37.67 ºN, 101.33 ºE	3358	Dense alpine meadow	2003-2010	Yu et al., 2006
HBG-W01	ChinaFLUX Haibei wetland	37.61 ºN, 101.33 ºE	3357	Alpine wetland	2004-2009	Zhang et al., 2020
CN-Ha2	FLUXNET Tibet Haibei Alpine	37.37 ºN, 101.18 ºE	3824	Alpine meadow	2002-2004	Kato et al., 2004
CN-Hgu	FLUXNET-CH4 CN-Hgu Hongyuan	32.85 ºN, 102.59 ºE	3500	Alpine meadow	2015-2017	Niu and Chen, 2020
MQ	Maqu site	33.89 ºN, 102.14 ºE	3423	Dense alpine meadow	2013-2016	Shang et al., 2015
Namco	Namco site	30.89 ºN, 90.24 ºE	4760	Alpine steppe	2019-2021	this study

2.2.1 ET products

This study examined 22 ET datasets (including 20 global datasets and 2 regional datasets) (Table 2), and detailed descriptions of each ET data can be found in SI in Supplementary materials. Among these datasets, 7 datasets were with high spatial resolution (≤1km), including ETMonitor (Zheng et al., 2022), MOD16 (Mu et al., 2011), MOD16-STM (Yuan et al., 2021), the Penman–Monteith–Leuning Version 2 (PMLV2) (Zhang et al., 2019), the operational Simplified Surface Energy Balance (SSEBop) (Senay et al., 2020), GLASS (Yao et al., 2014), and SynthesisET (Elnashar et al., 2021). Most of these high-resolution ET datasets used the different variables or indices from Moderate Resolution Imaging Spectroradiometer (MODIS) as main inputs. Two products (GLASS, SynthesisET) are ensemble ET products generated by fusing other ET models or datasets. Remote sensing ET datasets with coarse resolution were also collected, including Thermal Energy Balance (EB) ET (Chen et al., 2021), Breathing Earth System Simulator version 2 (BESSv2) (Li et al., 2023), GLEAM (version 3.5a based on satellite and reanalysis data with long-term coverage, and version 3.5b based on mainly satellite data) (Martens et al., 2017), and FLUXCOM (RS version using MODIS remote sensing data as input, and RS_METEO version using remote sensing and meteorological data as input) (Jung et al., 2019). MOD16-STM and PMLV2-Tibet are regional ET datasets that were calibrated against ground-based eddy-covariance measurements on the TP. MOD16-STM is an enhanced version of the MOD16 algorithm by redefining the transpiration and soil evaporation module (Yuan et al., 2021), while PMLV2-Tibet is a calibrated version of PMLV2 (Ma and Zhang, 2022). We also collected some ET products based on land surface models and climate reanalysis datasets, including calibration-free complementary relationship (CR) ET (Ma et al., 2021), TerraClimate (Abatzoglou et al., 2018), MERRA2 (Gelaro et al., 2017), ERA5 (Hersbach et al., 2020), ERA5-Land (Muñoz-Sabater et al., 2021), GLDAS-VIC (Rodell et al., 2004), GLDAS-Noah (Rodell et al., 2004), GLDAS-SLSM (B. Li et al., 2019).

Table 2: List of ground flux tower observation sites.

Products	Temporal resolution	Spatial resolution	Temporal coverage	Basic principle and approach	Validation method	Reference

https://doi.org/10.5194/hess-2024-55
Preprint. Discussion started: 13 March 2024

ETMonitor	Daily	1km	2000-2021	ETMonitor model with multi-parameterizations for different processes including plant transpiration, soil evaporation, evaporation from canopy intercepted rainfall and open water body, sublimation from snow/ice	Both ground observation and water balance estimation	Zheng et al. 2022
MOD16	8-day	500m	2000-present	MOD-PM based algorithm for vegetation covered region	Both ground observation and water balance estimation	Mu et al. 2011
PMLV2	8-day	500m	2002-2019	Penman-Monteith-Leuning model V2 using remote-sensing as input	Both ground observation and water balance estimation	Zhang et al. 2019
SSEBop	10-day	1km	2002-2019	Operational Simplified Surface Energy Balance using satellite psychrometric principle	Both ground observation and water balance estimation	Senay et al., 2020
GLASS	8-day	1km	2000-2018	Bayesian multi-model ensemble of different ET products	Both ground observation and water balance estimation	Yao et al. 2014
SynthesisET	Monthly	1km	1982-2019	Synthetization of different ET products based on ranking of validation metrics	Both ground observation and water balance estimation	Elnashar et al. 2021
MOD16-STM	Monthly	1km	2000-2018	Enhanced MOD16 algorithm by redefining the transpiration and soil evaporation module	Both ground observation and water balance estimation	Yuan et al. 2021
PMLV2-Tibet	8-day	5km	1982-2016	Penman-Monteith-Leuning V2 model calibrated in Tibet Plateau	water balance estimation	Ma et al. 2022
EB	Monthly	0.05°	2000-2017	Improved Surface Energy Balance method based monthly LST	water balance estimation	Chen et al. 2021
BESSv2	monthly	5km	1982-2019	Quadratic form of the Penman-Monteith equation to estimate ET uses various satellite remote-sensing as input	water balance estimation	Li et al. 2023
FLUXCOM-RS	8-day	0.0833°	2001-2015	FLUXNET and ensemble multiple machine learning	water balance estimation	Jung et al. 2019
FLUXCOM-RS-METEO	8-day	0.5°	2001-2013	FLUXNET and ensemble multiple machine learning	water balance estimation	Jung et al. 2019
GLEAM3.5a	Daily	0.25°	1980-2018	Priestley-Taylor equation and data assimilation of soil moisture	water balance estimation	Martens et al. 2017
GLEAM3.5b	Daily	0.25°	2003-2018	Priestley-Taylor equation and data assimilation of soil moisture	water balance estimation	Martens et al. 2017
CR	Monthly	0.25°	1982-2018	calibration-free complementary relationship model	water balance estimation	Ma et al. 2021

https://doi.org/10.5194/hess-2024-55
Preprint. Discussion started: 13 March 2024

Hydrology and Earth System Sciences Discussions

TerraClimate	Monthly	0.25°	1958-2020	modified Thornthwaite-Mather climatic water-balance model	water balance estimation	Abatzoglou et al., 2018
GLDAS-CLSM	Daily	0.25°	2003-present	Global Land Data Assimilation System，Catchment Land Surface Model (GLDAS_CLSM025_DA1_D.2.2)	water balance estimation	B. Li et al., 2019
GLDAS-Noah	Monthly	0.25°	2000-present	Global Land Data Assimilation System Version 2， Noah Land Surface Model (GLDAS_NOAH025_3H.2.1)	water balance estimation	Rodell et al., 2004
GLDAS-VIC	Monthly	1°	2000-present	Global Land Data Assimilation System Version 2.1， Noah Land Surface Model (GLDAS_VIC10_3M.2.1)	water balance estimation	Rodell et al., 2004
MERRA2	Monthly	0.25°	1979-present	the Modern-Era Retrospective analysis for Research and Applications, Version 2	water balance estimation	Gelaro et al., 2017
ERA5	Monthly	0.25°	1979-present	fifth generation of European ReAnalysis of ECMWF	water balance estimation	Hersbach et al., 2020
ERA5-Land	Monthly	0.25°	1979-present	new land component of the fifth generation of European ReAnalysis of ECMWF	water balance estimation	Muñoz-Sabater et al., 2021

2.2.3 Water balance-based ET data

We also collected water balance-based evapotranspiration (ET_{wb}) from other studies at the basin-scale to evaluate the accuracy of ET data products. Compared with the flux tower data, ET_{wb} can also be used to validate these products with coarse spatial resolution (≥5km). The monthly ET_{wb} may also involve uncertainties because of the propagated errors from precipitation and water storage, although ET_{wb} is often considered as 'ground truth' for validating basin-wide ET estimates. Totally, monthly ET_{wb} from five river basins were extracted from previous studies (Ma and Zhang., 2022; Wang et al. 2021), including the headwaters of Yellow basin, headwaters of Yangtze basin, upper Heihe basin, and two endorheic basins (Inner Tibet Plateau, Qaidam basins), as shown in Figure 1.

2.2.4 Other data

The precipitation data adopted in this study is from TPHiPr dataset, which is a long-term high-resolution (1/3°, daily) precipitation for the TP by merging the atmospheric model output with gauge observations from more than 9000 rain gauges around TP (Jiang et al. 2023). Compared to other widely used precipitation datasets, this dataset has remarkably better accuracy in TP, with generally unbiased and root mean square error of 5.0 mm/d.

The leaf area index (LAI) data is from the Global Land Surface Satellite (GLASS) data products (Xiao et al., 2014, 2022). GLASS LAI has a spatial resolution of 500m, which were spatially aggregated to 1-km resolution in this study.

The effect of net radiation (Rn) on ET is explored. The grid Rn data used in this study were obtained from Zheng et al. (2022), which calculated Rn as the difference between incoming and outgoing radiation fluxes both in shortwave and longwave based on mainly GLASS albedo and ERA5 data. The adopted Rn has an RMSE value of 30.75 W/m^2 when validated against ground

https://doi.org/10.5194/hess-2024-55
Preprint. Discussion started: 13 March 2024


Hydrology and Earth System Sciences
Discussions

measurements (Zheng et al. 2022), which is comparable to the RMSE of 33.56 W/m^2 for CERES (Clouds and the Earth's Radiant Energy System) Rn products (Jia et al., 2016).

2.3 Methodology

2.3.1 ET products validation

We fist validate the ET from different products (refer to Table 2) against ground observations and basin-scale water balance, and various accuracy indicators were calculated to assess the performance of these ET datasets. These ET datasets were selected as the mainstream gridded ET products obtained by a variety of typical algorithms applied in TP or globally. Considering the footprint of *in-situ* flux tower observations was generally within several hundred meters to kilometers, they were adopted to validate ET at relatively high resolution (≤1km) including six global ET products and one regional ET products, including ETMonitor MOD16, PMLV2, SSEBop, GLASS, SynthesisET, and MOD16-STM, while all products were validated based on the basin-scale water balance estimation. When validating with ground observations, ET values from the pixels where the flux sites are located were directly extracted for comparison. When comparing with ET_{wb} data, basin-scale monthly averaged ET by different products were calculated using area-weight average method according to the basin boundary.

The following commonly used accuracy indicators are employed, including the correlation coefficient (R), the bias, the root mean square error (RMSE), and the Kling-Gupta efficiency (KGE) (Gupta et al., 2009). KGE is a multi-objective statistical indicator incorporating the correlation, relative variability ratio and mean values ratio, to assess the performance comprehensively. KGE was calculated as:

$$KGE = 1 - \sqrt{(R-1)^2 + (\frac{\mu(ET_e)}{\mu(ET_o)} - 1)^2 + (\frac{\sigma(ET_e)}{\sigma(ET_o)} - 1)^2}\,, \quad (1)$$

where ET_e (mm/month) indicates the ET values of different products, ET_o (mm/month) indicates the ground-truth ET values, either from in-situ observations or basin-scale water balance estimation, μ is the mean value, σ is the standard deviation, and R is the Pearson correlation coefficient between the ET values and the ground-truth ET values. KGE is smaller than 1, and higher KGE means better agreement between the observed and the simulated results generally.

2.3.2 Inter-comparison of different products

To inter-compare the spatial variation of ET by different products, multiple-year averaged annual ET was estimated for each product during their overlap period (2003 ~ 2015). The averaged and median values of ET, as well as the stand deviation, by different products were estimated at both pixel-wise and basin-wise level, to express the discrepancy of ET magnitude by different products. The ratio of standard deviation to multi-products averaged ET values was estimated to present the uncertainty. For products that also provide the ET components, including plant transpiration, soil evaporation, canopy rainfall

https://doi.org/10.5194/hess-2024-55
Preprint. Discussion started: 13 March 2024


Hydrology and Earth System Sciences Discussions

interception evaporation, open water evaporation, and snow/ice sublimation, the separate contribution of these components to total ET are also calculated and compared.

To compare the seasonal variation of ET, monthly climatology was produced by calculating the mean value for each month for each product. It is generally agreed that long-term coverage (i.e., at least 30 years) is required when analyzing the trend of climate variables. However, most ET products cover a relatively short period in this study. Although the relative short period of time may be debated, the trend of annual ET by each product was detected using robust regression to compare the annual variation of ET by different products.

2.3.3 Response of ET to different environmental factors

To investigate the impact of environmental factors on the variation of ET, the Pearson correlation analysis was conducted to measure how annual ET responds to its main governing environmental factors, including precipitation, LAI, and net radiation. These variables were selected to represent the strength of the water cycle, energy budget, and plant physiology, which are the three main processes regulating ET.

3. Results

3.1 Evaluation of ET products

3.1.1 Validation of ET products against flux tower measurements

Figure 2 and Supplementary Figure S2 present the validation results. It should be noticed that all the products have different temporal and spatial coverage, e.g., the MOD16 ET product does not provide data in non-vegetation covered pixels (hence no MOD16 ET data for sites of QOMS and NADORS), and the validation results are obtained primarily based on a different number of samples for different products. To have a fairer comparison, Figure 2 also shows the indicators when using same validation samples for all the products, which was conducted by limiting the validation samples only at the vegetation covered sites during 2001~2018.

As anticipated, the regional ET product (MOD16-STM) demonstrated good accuracy with low RMSE and high KGE (15.84mm/month and 0.77 when using the same validation samples). This may be attributed to the fact that MOD16-STM ET was calibrated using the flux observation and was retrieved based on the regional bias-corrected climate data with better accuracy than the global forcing data. Among all the global ET datasets, ETMonitor and PMLV2 ET achieved the highest accuracy with the highest KGE (>0.77) and lowest RMSE (<20mm/month), which was comparable to the MOD16-STM ET product. Most products showed better accuracy at the relatively wet sites with dense vegetation (e.g., GT, HBG, ARS, CN-Ha2), judged by relative higher values of KGE and R, than at the relatively dry sites with sparse vegetation or desert (e.g., QOMS, NADORS). The SSEBop product exhibited the largest negative bias and lowest KGE for relative wet sites and desert

https://doi.org/10.5194/hess-2024-55
Preprint. Discussion started: 13 March 2024

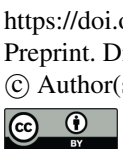

Hydrology and Earth System Sciences
Discussions

sites, but showed good accuracy for some alpine steppe sites with sparse vegetation (e.g., SH, YK, NAMORS). Figure 2 also indicates that the ensemble ET datasets (GLASS and SynthesisET) did not exhibit better accuracy than others, e.g., both with low KGE (both less than 0.6) and large negative bias (-13.76 ~ -10.82mm/month), which is most likely related to the ensembled data sources and algorithms.

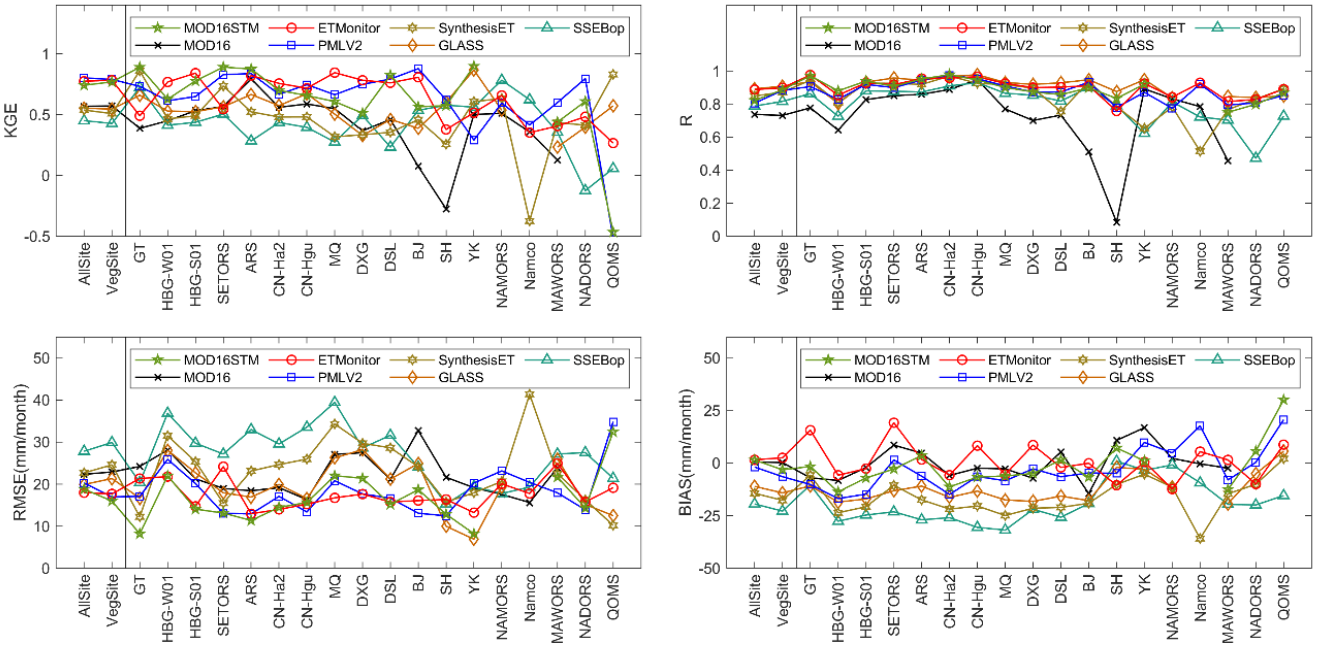

Figure 2: Summary of the validation results of high-resolution ET products against flux tower measurements. *AllSite* indicates that the validation results are obtained based on different samples depending on the availability of each product, while *VegSite* represents the validation results are obtained based on same sample numbers (mainly vegetation covered sites during 2001~2018) for every product.

3.1.2 Evaluation of ET products against water balance model estimates

Figure 3 and Supplementary Figure S3 show the comparison between all ET products with the basin-scale water balance ET (ET_{wb}). As anticipated, the regional ET products (MOD16-STM and PMLV2-Tibet) showed good accuracy, with KGE of 0.64~0.87 and RMSE of 12.19~15.60 mm/month. Although both MOD16-STM and PMLV2-Tibet were calibrated using the ground flux observations in TP, their performance differed with MOD16STM ET showed slightly lower KGE, most likely due to its relative underestimation when ET values were high (Figure 3 and Supplementary Figure S3). ETMonitor and PMLV2 ET also showed high KGE (≥0.80) and low RMSE (<14mm/month). SynthesisET produced the highest RMSE and BIAS, which is because SynthesisET ensembles different data sources during different periods, resulting in time series inconsistency. Among the reanalysis and LSM ET products with coarse resolution, TerraClimate, ERA5, and ERA5-Land showed overall

https://doi.org/10.5194/hess-2024-55
Preprint. Discussion started: 13 March 2024

Hydrology and Earth System Sciences
Discussions

good accuracy with KGE≥0.78 and RMSE≈13 mm/month, while GLDAS-CLSM and GLDAS-VIC exhibited large errors with RMSE≥20 mm/month and KGE≤0.41. CR also showed overall good accuracy in TP but had relatively lower KGE in arid basins (e.g., InnerTP), where GLEAM and SSEBop showed relatively higher KGE. Among all the products, the PMLV2-Tibet and ETMonitor ET products showed lowest RMSE (<13mm/month) and highest KGE (0.87) and R (>0.90) when comparing with ET_{wb}. The global ET products with above-average accuracy include ETMonitor, PMLV2, GLEAM35a, GLEAM35b, TerraClimate, ERA5, and ERA5Land, judged from their lower RMSE and higher KGE. When regressed against ET_{wb}, most ET products showed slope values less than one, indicating these ET products tend to underestimate ET in regions or periods with high ET values (Supplementary Figure S3). Among them, ETMonitor, CR, and TerraClimate ET showed slope values close to 1 (larger than 0.9), which highlights their good accuracy.

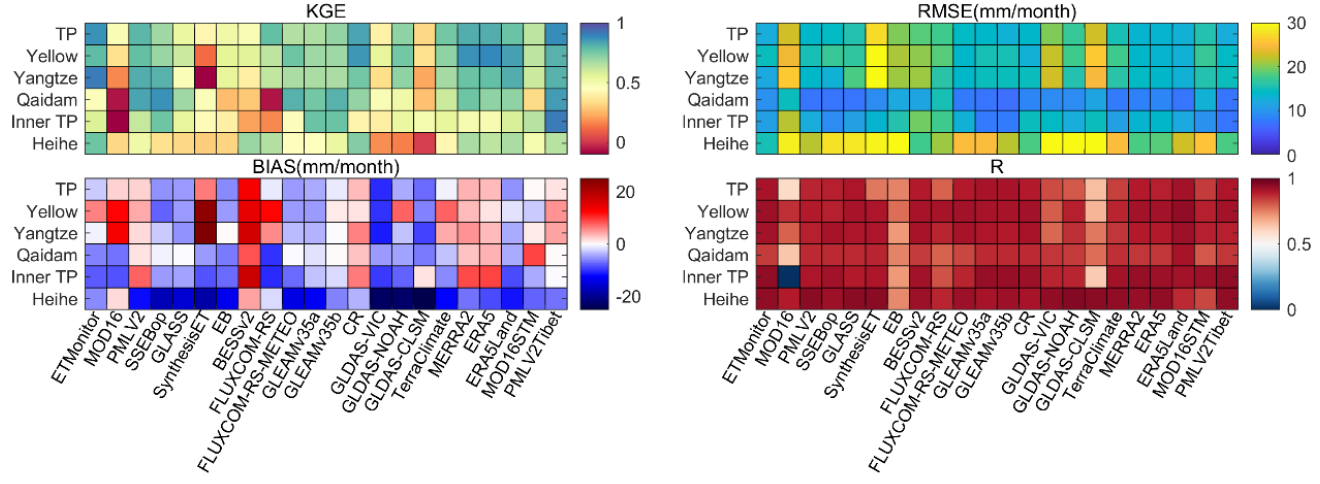

Figure 3: Summary of the validation results of ET products against basin-scale ET based on water balance modelling. TP presents the validation results when data from all five basins were adopted.

3.2 Variability of ET across the TP

3.2.1 Spatial variation in ET across TP

Figure 4 presents the spatial variation of multi-year averaged annual ET across TP by different products. The mean value of the 22 ET products and the standard deviation are also displayed in Figure 4. In general, most of the products indicated pixel-wise ET values lower than 800mm/yr and presented a similar spatial pattern, with high ET values in the eastern part and low ET in the western TP. The pixel-wise ET histogram showed two peaks for some datasets, e.g., ETMonitor, EB, MERRA2. These peaks correspond to the low ET values of non-vegetation or sparsely-vegetated regions in the middle and western TP and high ET values of regions in the eastern TP with dense vegetation and relative humid climate. The spatial variations of the standard deviation of different products is also shown in Figure 4, and large differences among different products in the middle-

https://doi.org/10.5194/hess-2024-55
Preprint. Discussion started: 13 March 2024

Hydrology and Earth System Sciences
Discussions

to-west TP can be noticed, where some ET products show low ET values (e.g., ET values from ETMonitor, SSEBop, EB, are generally less than 200mm/yr) while some ET products show much higher ET values (e.g., ET values from BESSv2, CR, and ERA5 reach 400mm/yr).

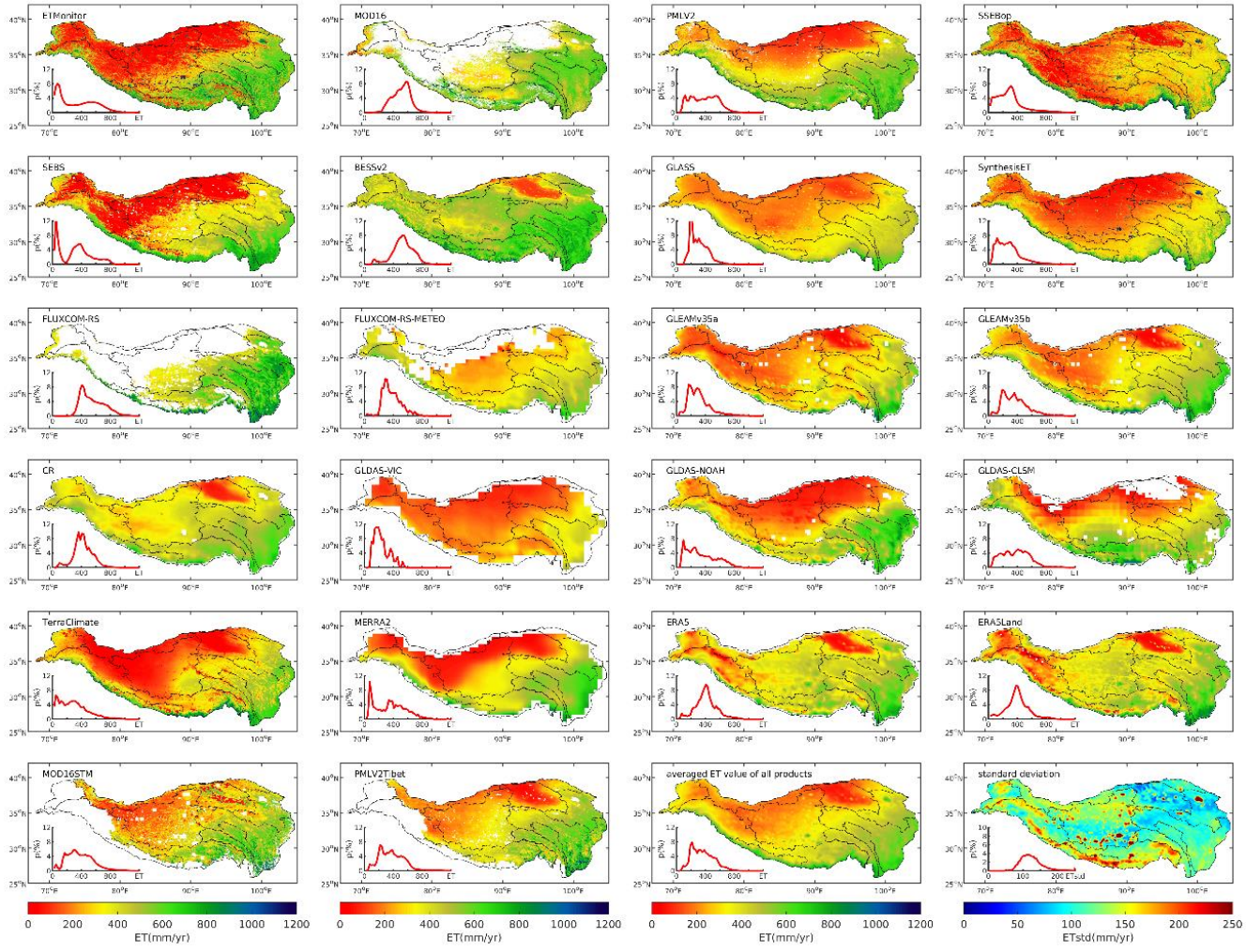

Figure 4: Spatial variation of ET in Tibetan Plateau by different products during their overlap period (2003~2013). The inset in each panel shows the histogram of ET values.

Figure 5 summarizes the multiple-year averaged ET in TP and different basins using different products. It should be noted that some products only provide ET values for the vegetation-covered regions, e.g., MOD16, FLUXCOM-RS and FLUXCOM-RS-Meteo, and their ET shown here are obtained only based on the available data. Among all the ET products, BESSv2 ET presents highest multiple-year averaged ET value in TP, while GLDAS-VIC shows the lowest ET values (Figure 5). According to the evaluation results mentioned above, seven ET products (ETMonitor, PMLV2, GLEAMv3.5a, GLEAMv3.5b, TerraClimate, ERA5, and ERA5Land) were found to have continuous spatial coverage and provide accurate estimates, and the

https://doi.org/10.5194/hess-2024-55
Preprint. Discussion started: 13 March 2024

Hydrology and Earth System Sciences
Discussions

median and average annual ET by these products in the TP are 362.21 mm/yr and 350.34 mm/yr, respectively, with a standard deviation of 42.46 mm/yr. Based on the TPHiPr precipitation data (Jiang et al., 2023), the total annual precipitation in the TP is 631 mm/yr, therefore ET accounts for roughly 55(±7)% of the annual total precipitation. The difference among these products also noticeable at the basin scale. The basins with low ET and sparse vegetation cover (e.g., Qaidam, Inner Plateau, Hexi Corridor, Tarim, and Amu Darya) exhibit the largest inter-product uncertainty, expressed as the ratio of standard deviation to the averaged values (Supplementary Table S1). The uncertainty in the Indus basin and Brahmaputra basin is also high, most likely due to their complex topography, extreme high elevation, and large coverage of permanent glaciers and snow, which make it difficult to achieve reliable estimates.

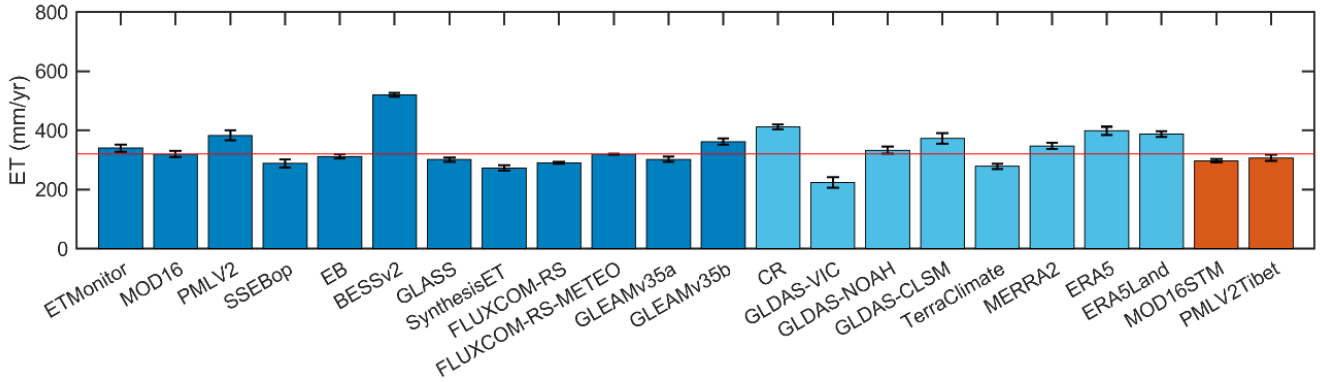

Figure 5: Bar plot of the multiple year (2003~2013) averaged ET in Tibetan Plateau by different products. The red horizontal line represents the average ET of all products.

3.2.2 Temporal variations in ET across TP

Figure 6 presents the monthly variation of ET across TP, while Supplementary Figure S4 illustrates the difference between different products. Despite the varying different shapes observed, most products indicate that the highest ET occurs in July and August. ET during the monsoon season (June to September) and pre-monsoon season (March to May) accounts for 62% (±7%) and 23% (±4%) of the annual total ET, respectively. The remaining 15% of ET occurs during October to next February. As a comparison, 66% and 22% of the annual total precipitation occurs during the monsoon and pre-monsoon seasons, while the remaining 12% occurring during the rest of the year. The monthly patterns of ET variations are similar across all basins, with differences in magnitude. The proportion of ET during the monsoon season is higher in dry basins, e.g., 69% in Hexi Corridor and 68 % in Qaidam, compared to the wet basins, e.g., 53% in Ganges and 58% in Brahmaputra.

https://doi.org/10.5194/hess-2024-55
Preprint. Discussion started: 13 March 2024

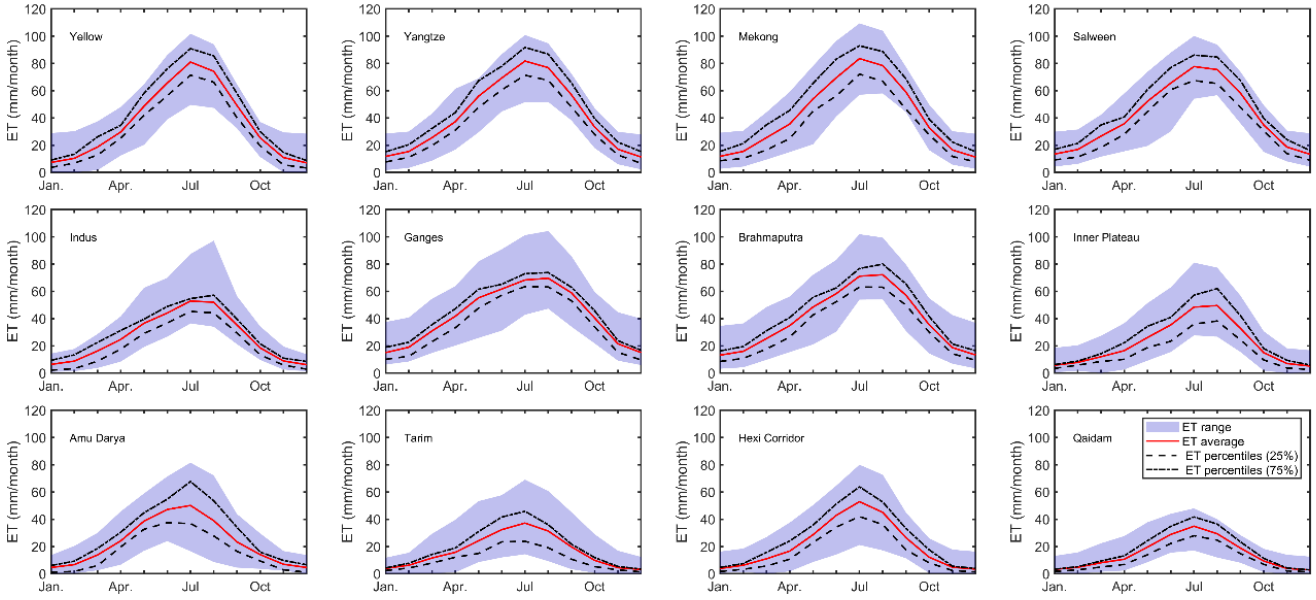

Figure 6: Seasonal variation of ET in different basins in Tibetan Plateau. Data shown are monthly averaged ET value of during 2003~2013.

Figure 7 presents the yearly variation of ET across TP for different products. Large deviations were observed among products, with CR and ERA5 having the largest value of averaged ET while the GLDAS-VIC has the lowest. The trend of annual ET varies with different products and their temporal coverage (Figure 7 and Supplementary Figure S5). The results suggest a general increasing trend of ET since the 1980s. Since 2000, the annual ET has showed both positive and negative trends depending on the product. Most products showed increasing trend, and the median ET of all products increased at a rate of 1.70 mm/yr from 2000 to 2020 in TP. The SynthesisET showed the largest negative trend due to its temporal inconsistency. At the basin scale, the difference in annual trends among different products is also clearly illustrated (Supplementary Figure S5). Most basins are experiencing an increasing trend of ET, particularly the Yellow, Yangtze, Mekong, Tarim, Hexi Corridor, Tarim, and Qaidam basins, where most products had a positive ET trend. The median values of ET trend are either negative or close to zero in Ganges, Brahmaputra, Amu Darya, and Inner Plateau, which probably indicates a decreasing or non-monotonic trend for these basins.

https://doi.org/10.5194/hess-2024-55
Preprint. Discussion started: 13 March 2024

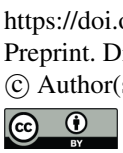

Hydrology and Earth System Sciences
Discussions

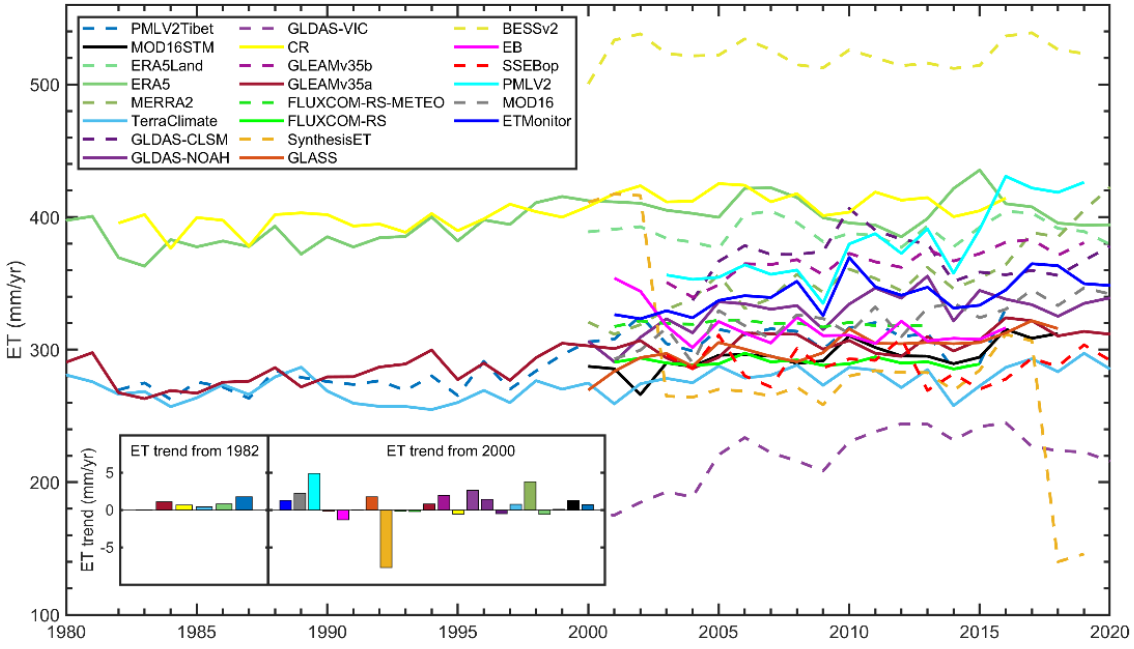

Figure 7: Yearly variation of ET in Tibetan Plateau by different products. The inset panel shows the annual ET trend by different products.

3.2.3 ET components

Among these products, there are nine that provide the main components of ET (Ec, Es, and Ei), including ETMonitor, PMLV2, MOD16STM, GLEAMv35a, GLEAMv35b, GLDAS-VIC, GLDAS-NOAH, GLDAS-CLSM, and MERRA2. It is important to note that there is no independent reference available for the ET components, and each model has a distinct way of estimating these components. Even when the total ET is consistent across various products, the individual components can differ significantly (Figure 8 and Supplementary Figure S6). All products show higher Ec and Ei values in the eastern TP and lower values in the middle and western TP. This pattern follows the spatial distribution of environmental factors (e.g., LAI and precipitation), i.e. regions with high ET values are mostly covered by forest and alpine meadow with higher precipitation, while regions with low ET values are dominated by where sparse vegetation (alpine steppe and desert steppe) with lower precipitation. Large deviations were observed in Es values, with several products exhibiting high Es values in the eastern TP, e.g., MERRA2, GLDAS-CLSM, ETMonitor, and MOD16STM, while some products showed extremely low Es values, e.g., GLEAMv35a, GLEAMv35b, and GLDAS-VIC.

Figure 8 presents the false color composite maps of the relative magnitude of transpiration (Ec), soil evaporation (Es), and interception (Ei) by different products, with Red (Es is largest), Green (Ei is largest), Blue (Ec is largest). In the false color composite maps, the red (green, blue) color means that Es (Ei, Ec) contributes most to total ET. Clear differences exist among

https://doi.org/10.5194/hess-2024-55
Preprint. Discussion started: 13 March 2024

Hydrology and Earth System Sciences
Discussions

different products. Most products generally suggest that Es contributed most to the total ET. In contrast, three products (GLEAMv35a, GLEAMv35b, and GLDAS-VIC) show that plant transpiration is the primary contributor to total ET, mostly likely caused by their extreme low Es values in eastern TP by these three products (Supplementary Figure S6). The averaged Es/ET values range from 18% by GLDAS-VIC to 84% by MOD16STM, with a median value of 50%. The averaged Ec/ET values range from 11% by GLDAS-CLSM to 58% by GLEAMv35a, with a median value of 30%. Most products generally showed low Ei/ET values with a median value of 5%, while GLDAS-VIC and GLDAS-NOAH exhibit the highest Ei/ET value (20% ~ 36%).

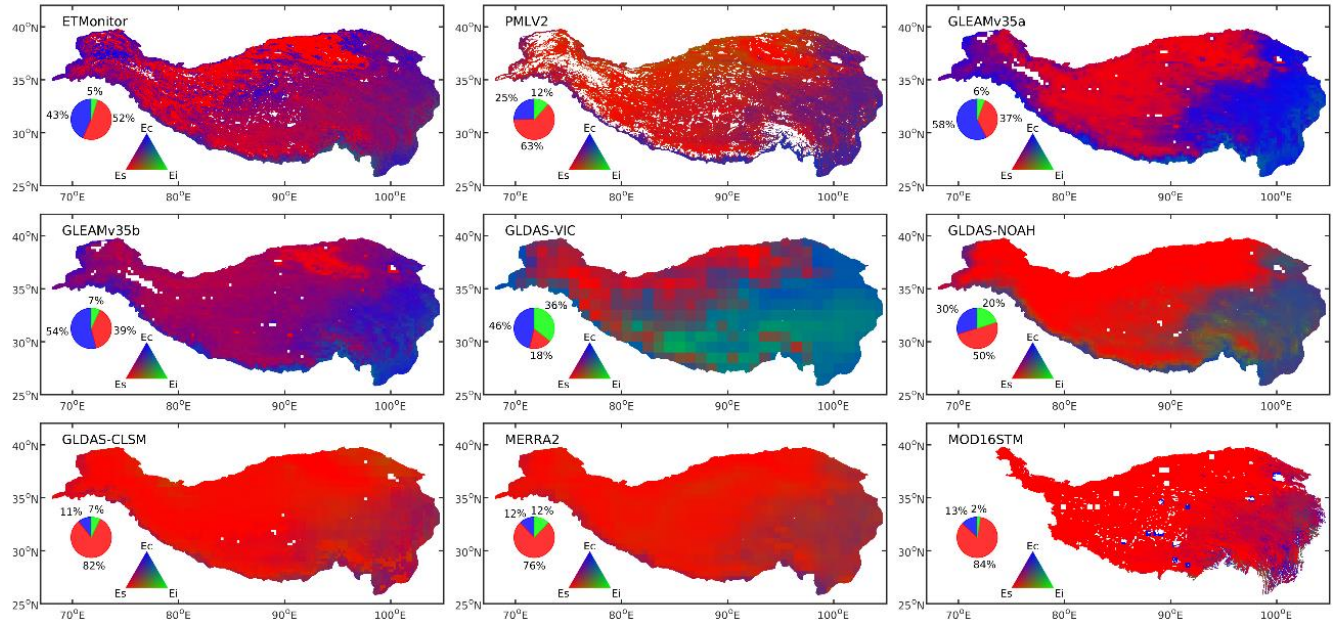

Figure 8: False color composite maps to visualize the relative magnitudes of the transpiration (Ec), soil evaporation (Es), and interception (Ei) contribution to total ET according to different products.

In addition, two other components of water vapour flux are considered separately: evaporation from open water bodies (Ew) and sublimation from snow/ice-covered surfaces (Ess). There are three products providing open water evaporation, including ETMonitor, GLEAMv35a and GLEAMv35b (Figure 9), and five products providing snow/ice sublimation, including ETMonitor, GLEAMv35a, GLEAMv35b, GLDAS-CLSM, and MERRA2 (Figure 9). For open water evaporation, three products provide comparable Ew results with average Ew/ET from 3.45% to 4.10%. For snow/ice cover surface sublimation, GLDAS-CLSM provided the overall highest Ess/ET value with a regional average of 7.79% and GLEAMv35a provided the overall lowest Ess/ET value with a regional average of 1.20%. This difference is mainly caused by large differences of Ess among different products in the southern TP, e.g., in the Indus, Ganges and Brahmaputra watersheds, where Ess is not well captured by GLEAM. ETMonitor's Ess falls in the middle of these extremes, with a regional average of 4.3%.

https://doi.org/10.5194/hess-2024-55
Preprint. Discussion started: 13 March 2024

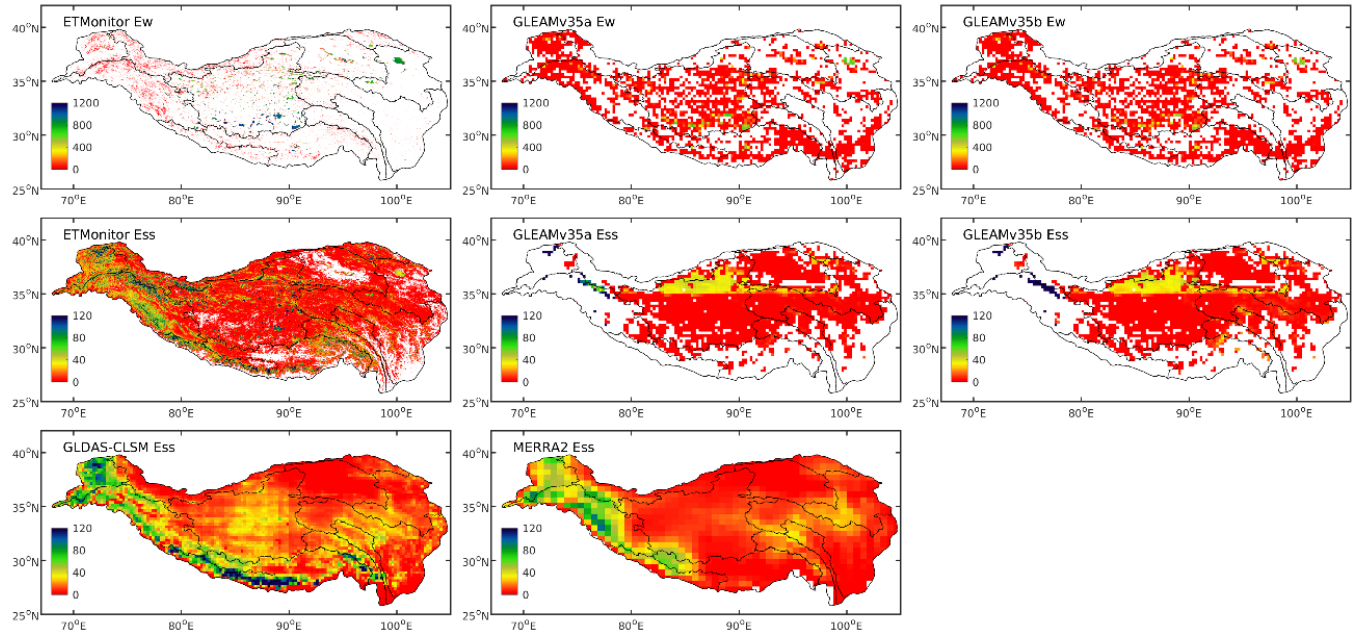

Figure 9: Spatial variability of open water evaporation (Ew) and snow/ice sublimation (Ess) in Tibetan Plateau by different products.

3.3 Response of annual ET to the main governing environmental factors

Figure 10 shows the pixel-wise median R values of all ET products with precipitation, Rn, and LAI. A negative R value was obtained when ET exhibited an opposite annual trend to the regulation effect. ET and precipitation showed high positive R in the water-limited middle and northern part of TP (e.g., Inner Plateau, Qaidam, Hexi Corrida, Yellow), while they showed negative R in the southeast part of TP (e.g., Yangtze, Mekong, Salween, Brahmaputra) with high precipitation and limited energy due to cloudiness. ET had positive correlation with Rn in the northern part of TP (the water-limited regions, e.g., Yellow, Qaidam, Hexi Corrida), however with smaller R than with precipitation. ET and Rn also showed positive correlation in the eastern part of TP (e.g., Yangtze, Mekong, Salween, Brahmaputra), indicating that energy plays a more important role than water in regulating the variability of ET in these regions. Conversely, ET and Rn showed negative correlation in the middle part of TP (e.g., Inner Plateau) since this region is mainly water-limited. The correlation between ET and LAI is generally weak, however large positive R values could be found in the north and east part of TP (especially in the Yellow, Hexi Corride, and Qaidam) and occasionally in other areas. It should be noticed that plants tend to grow more (higher LAI) with more water available in the water-limited regions (e.g., Inner TP), and higher correlation between ET and LAI in these regions may also be associated with the governing effect of water. In the energy-limited regions, e.g., Mekong and Salween, higher LAI may result in higher Rn due to the generally lower albedo of plant compared to soil, which reduces the effect of Rn.

https://doi.org/10.5194/hess-2024-55
Preprint. Discussion started: 13 March 2024

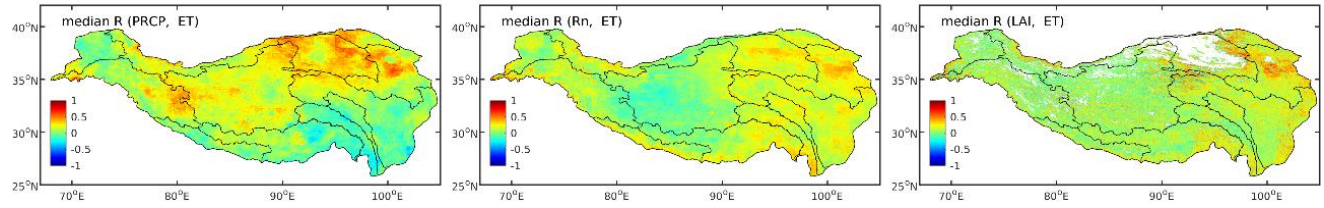

Figure 10: The spatial variation of the median correlation coefficient (R) of ET with precipitation, Rn, and LAI.

Supplementary Figure S7 presents the variables that showed the highest absolute R, with red (green, blue) colors means that Rn (LAI, precipitation) has a highest temporal correlation. This allows for an easy visualization of the most important factors governing ET according to different products. The differences in R values are closely related to the biophysical nature of each algorithm, and are mostly likely associated with the algorithms and the drivers. For instance, GLEAM products utilize surface soil moisture data as input and simulate root zone soil moisture relied on precipitation to account for the impact of available surface water on ET, and the estimated ET were strongly correlated with precipitation, especially in the Inner Plateau region. The difference caused by the drivers are also emphasized, especially when comparing GLEAMv35a and GLEAMv35b, which were produced based on same algorithms but different drivers (Mentens et al., 2017).

4. Discussions

To understand the regional and global climate change, as well as regional ecohydrological processes in the TP, it requires knowledge of the changes in ET over time and space. This study evaluated 22 ET products using various methods, e.g., comparing ET products with ground EC observations and basin-scale water balance estimations, assessing the spatiotemporal variability of ET and its components, and exploring the response of ET in TP to environmental factors, to assess the performance of ET products and clarify the ET amount and variability in the TP. After these comprehensive evaluation and analysis, we have gained a clear understanding of the water vapour released by TP. Additionally, we notice that evaluation results are highly relevant to the ET model and the considered vaporization processes, and provide suggestions for further implications in ET estimation for TP. Among the evaluated ET products, there are 14 products that primarily use remote sensing products, including 2 products (SSEBop and EB) based on land surface temperature (LST), 8 products (ETMonitor, MOD16, MOD16-STM, PMLV2, PMLV2-Tibet, GLEAMv35a, GLEAMv35b, BESSv2) based on PM-types models (including Penman-Monteith equation, Priestley-Taylor equation, Shuttleworth-Wallace equation), 4 products (FLUXCOM-RS, FLUXCOM-RS-METEO, GLASS, SynthesisET) based on data-driven methods.

https://doi.org/10.5194/hess-2024-55
Preprint. Discussion started: 13 March 2024


Hydrology and Earth System Sciences
Discussions

4.1 Relevance of validation results with vaporization processes

4.1.1 Processes captured by tower-based observation using eddy covariance system

The *in-situ* observation by eddy covariance system is recognized as the standard method for monitoring energy and mass fluxes to validate high-resolution ET (Baldocchi, 2020). The eddy covariance system observation represents the net water flux integrated across different processes (e.g., plant transpiration in the dense vegetation regions, snow sublimation during the dry snow cover periods, evaporation of canopy-intercepted water when the canopy is wet due to intercepted rainfall). The vaporization process observed by the eddy covariance system depends on the land surface condition, which may vary seasonally and yearly due to factors such as snow/ice, intercepted water, and vegetation. However, many ET products (e.g., MOD16 and PMLV2) assume a constant land surface condition throughout the year, which indicate that they cannot capture the temporal transitions of these vaporization process associated with changes in land cover. In contrast, ETMonitor adjusts the daily land cover inputted to the algorithm based on seasonal land cover condition (water cover and snow/ice cover), which enable it to partly reflect the impact of seasonal water cover and snow/ice cover on total ET (Zheng et al., 2022).

Meanwhile, eddy covariance system observation includes condensation when negative latent heat flux occurs. Remote sensing-based ET products mainly focus on positive ET (positive upward latent heat flux) and omit processes such as condensation. For example, in MOD16 ET product algorithm, Rn was mandatory to positive (Rn was set to 0 if Rn<0) indicating that negative ET is not allowed. Negative ET (e.g., condensation) may also occur when VPD is negative. Depending on whether negative Rn or negative VPD is allowed, the considered water phase changes differs, and it surely will impact the performance of ET products.

4.1.2 Validation results based on basin-scale water balance method

The validation results using the basin water balance method show generally consistent results and slightly superior evaluation metrics compared to the flux tower validation results. This may be attributed to the representation disparity between the flux tower measurements and the basin-scale ET_{wb} estimate. ET_{wb} is obtained at the basin scale (several hundred km^2), which is much larger than the footprint of flux tower observations (roughly km^2 depending on meteorological conditions). Basin-scale ET_{wb} may offset the positive and negative biases within the basin, resulting in better evaluation metrics. Considering the relative sparse distribution and small footprint of the flux-tower based eddy covariance system observation, the water balance method can serve as a useful complementary method for validating ET, which is especially true for the coarse-resolution ET that have much large spatial representation than eddy covariance system observations. However, it should also acknowledge the uncertainties in the water balance method as ground-truth data. This method is based on the validity of several assumptions (e.g., negligible subsurface leakage to adjacent basins) and the reliability of precipitation, runoff, and water storage (Mao et al., 2016). In the cold regions like the TP, where glaciers and snow have a substantial influence on the water balance, meltwater should also be considered (Wang et al., 2022).

https://doi.org/10.5194/hess-2024-55
Preprint. Discussion started: 13 March 2024


Hydrology and Earth System Sciences
Discussions

4.2 Implications for ET estimation in Tibetan Plateau

4.2.1 ET estimation using PM-type model

This study found that ET products generated using the PM-type model demonstrated superior accuracy compared to other models. In particular, ETMonitor and PMLV2 showed the highest accuracy in TP compared to both *in-situ* flux observations and basin-scale water balance estimated ET. This is consistent with the judgment that LST-based ET models are suited for water-limited conditions in bare and partially vegetated areas, while PM-type ET models are more effective for both energy-limited and water-limited conditions in vegetated areas (Chen and Liu, 2020). An exception was found for MOD16, which exhibited below-average accuracy overall, however its regional improved version (MOD16-STM) demonstrated significantly more accurate ET after regional parameter calibration and soil evaporation module enhancement (Yuan et al., 2021). The reason for this is that MOD16 only applies to limited areas and seasons of TP due to its incomplete parameterization, which fails to address the ET variation in the middle to western TP because it lacks estimation of bare soil and open water evaporation.

This study also highlights the potential for improving of parameterization or parameters for estimating ET using PM-based model, e.g., by incorporating soil moisture as water available stress or indicators, by integrating the water balance simulation and data assimilation, or by coupling with carbon cycle in simulating ET. We found that PM-type models that incorporated soil moisture to detect water stress produced very good results. For instance, to enhance the accuracy of estimated ET, ETMonitor utilized high-resolution soil moisture data to refine the soil resistance and canopy resistance parameterizations for plant transpiration and soil evaporation, and calibrated the most sensitive parameters based on ground observation (Hu and Jia, 2015; Zheng et al., 2022). GLEAM assimilated surface soil moisture to derive the water availability at the root zone, and applied it to determine the water stress (Miralles et al., 2011), which also showed good accuracy of ET in TP. Coupling ET estimation with the carbon cycle can also be helpful, e.g., PMLV2 adopted water-carbon cycle coupling to aid ET estimation (Zhang et al., 2019), since canopy conductance controls both transpiration and photosynthesis. The regional adaption of parameterization and better driven forces are also appreciated, and their benefit were clearly illustrated in this study that MOD16-STM and PMLV2-Tibet products showed better agreement with reference values than MOD16 and PMLV2. Furthermore, the PM-type model-based ET products (especially those based on duel-source or multi-source models) can provide different ET components, benefiting from its inherent advantage in expressing the biological and non-biological processes.

4.2.2 ET estimation using LST-based model

Although the absolute accuracy of LST-based EB and SSEBop products may be lower than that of ET products by the optimized PM-types models, they have some advantages, e.g., the close coupling of energy balance through sensible heat flux, good capability of representing the spatial variations of ET, especially for the high-resolution dataset. Previous study criticized that the LST-based models fail to produce temporally and spatially continuous ET fields under variable cloud conditions,

https://doi.org/10.5194/hess-2024-55
Preprint. Discussion started: 13 March 2024


Hydrology and Earth System Sciences
Discussions

which was significantly improved recently through the temporal upscaling technologies, advanced satellite observations (Ryu et al., 2012; Tang et al., 2017; Zhong et al., 2019). The relatively good performance of SSEBop at some sites (e.g., SH, YK, NAMORS) in this study also demonstrates the potential of LST-based models to achieve accurate ET estimation at arid sparse-vegetated regions.

4.2.3 Uncertainty propagation in data-driven ensemble ET products

The ET products based on data-driven models performed diverse in TP. GLASS and SynthesisET were both obtained based on ensemble different ET products, with GLASS adopting Bayesian averaging method and SynthesisET using a ranking-based method (Yao et al. 2014; Elnashar et al. 2021). However, these two products exhibited significant differences, with SynthesisET showing much larger errors (Figure 3 and Figure 4). This finding on SynthesisET differ significantly from a previous study that validated ET product at global scale (Liu et al. 2023), which claimed that SynthesisET was the best product when applied in its time span based on accuracy indicators (e.g., RMSE) by comparing to in-situ observations and water-balance estimation. After screening the time series of SynthesisET, we found significant temporal inconsistency, mainly caused by its synthesis method. SynthesisET incorporated two or three high-ranked ET datasets in each time step according to the evaluation metrics, i.e., different products were adopted for different periods without correcting the inherent discrepancy of different products, which may be improved by advanced ensemble method or critical inputs selection (Wang et al., 2021). Therefore, to ensure a more reliable and comprehensive evaluation, we suggest addressing the evaluation in terms of spatial and temporal variation. Additionally, when conducting further data ensemble studies, it is important to properly consider the temporal inconsistency of different products.

Data-driven methods, especially the machine learning or deep learning methods, are increasingly applied in earth science to extract land surface parameters (Karpatne et al., 2017). The FLUXCOM product integrates the ET results upscaled from *in-situ* observations using various machine learning models (Jung et al. 2019). The FLUXCOM-RS-METEO product, which is obtained using both meteorological datasets and remote sensing datasets as driven forces, is found to have with comparable accuracy in TP. However, the FLUXCOM-RS product, which differ from FLUXCOM-RS-METEO that FLUXCOM-RS product is obtained without using meteorological datasets as driven forces, performs poorly in TP according to the validation in this study, indicating the importance of meteorological variables in estimating ET.

4.2.4 LSM and analysis ET products

We also compared various ET products by LSM and climate analysis, including GLDAS-Noah, GLDAS-VIC, GLDAS-CLSM, CR, TerraClimate, ERA5, ERA5Land, and MERRA2. Although these products generally have low spatial resolution (0.1˚~1.0˚), they have long-term temporal coverage, making them more suitable for climate analysis. Among them, TerraClimate, CR, ERA5, and ERA5Land showed overall good accuracy when compared with ET_{wb}, while GLDAS products yield relatively low accuracy. The performance of GLDAS ET datasets are mainly caused with the driven forces and parameter

https://doi.org/10.5194/hess-2024-55
Preprint. Discussion started: 13 March 2024


Hydrology and Earth System Sciences Discussions

settings, which need significant improvement when applying in TP (X. Li et al., 2019). In the middle and western regions of TP, where the surface vegetation cover is sparse and the climate is arid or semi-arid with very low precipitation (roughly 300mm/yr or less), CR, ERA5, and ERA5Land produce higher ET values than other products which exhibit lower ET values. The high ET values of ERA5 and ERA5Land are most likely due to the overestimated precipitation in TP by ERA5 (Jiao et al., 2021; Xie et al., 2022), which will also lead to overestimation of ET and runoff (Sun et al., 2021). Previous studies have reported the relatively high ET values by CR methods in middle and western TP (Yang et al., 2020) and Arctic basins (Ma et al., 2021), which can be explained by the uncertainty of the driven forces partly (Ma et al. 2021) and the applicability of CR in cold regions with complex energy processes (Yang et al., 2021). A basic assumption of CR is that the energy difference between apparent potential ET (ET_P) and wet environment ET has a linear or nonlinear relationship with the energy difference between ET_P and actual ET when water is limited, which fails during soil freezing and thawing periods when energy is used for the phase change of ice-water and sublimation (with much higher latent heat) (Yang et al., 2021). Furthermore, CR also assumes that the changes in land surface properties can be accurately and promptly detected from changes in atmospheric conditions, neglecting regional or large-scale advection, which makes it unapplicable in heterogeneous surfaces (Morton, 1983; Han and Tian., 2020 Crago et al., 2021).

4.2.5 Suggestions for further ET estimations in TP

To improve the ET estimation in TP, several aspects can be addressed. Current ET models could be improved by integrating different models and processes, e.g., combination of LST-based models and conductance-based PM-types models (Chen and Liu. 2020) or data-driven algorithms (Zhao et al., 2019; Shang et al., 2023), combination of ET processes with carbon cycle and hydrological processes (Zhang et al., 2019; Abatzoglou et al., 2018). Combining the PM-type models and machine learning algorithms in a proper way can inherit both advantages and result in a more powerful model for ET estimation (Koppa et al., 2022), and recent studies have highlighted the improved accuracy of the hybrid model by incorporating the machine learning methods estimated canopy conductance with PM-types equation for ET estimation (Zhao et al., 2019; Shang et al., 2023), which is another direction for further ET estimation in TP. Meanwhile, a main challenge in improving the ET algorithm or validating the estimation is the scarcity of the ground measurements, which highlight the need for the long-term comprehensive observations network in TP (Ma et al., 2020; Zhang et al. 2021). Furthermore, to improve the accuracy of the estimated ET, it is recommended to employ regionally optimized driving forces, e.g., climate reanalysis dataset that considers the specific climate of TP with higher accuracy and resolution (He et al., 2020).

4.3 Water vapor released by Tibetan Plateau

4.3.1 ET magnitude and variation in TP

This study confirms the large discrepancy in ET magnitude among various products, as previously reported in studies (e.g., Wang et al., 2020; W. Wang et al., 2018; X. Li et al., 2019). It also reveals substantial deviations in terms of spatiotemporal

https://doi.org/10.5194/hess-2024-55
Preprint. Discussion started: 13 March 2024


Hydrology and Earth System Sciences
Discussions

distribution of ET and ET components by different products. Our study suggests that the ET across TP ranges from 224mm/yr to 519mm/yr depending on the products used, with an average (median) value of 350.34 (362.21) mm/yr and a standard deviation of 42.46 mm/yr. ET accounts for roughly 55% of the annual total precipitation. This study mainly focuses on the vapor released into the atmosphere, while the downward vapor flux (mainly condensation) is not considered. A recent study based on ERA5 reanalysis data found that the annual mean condensation in TP is approximately 8.45mm/yr, which accounts for roughly 2% of the upward vapor flux (Li et al., 2022). The surface condensation is generally rare in glacier due to the continuous low temperature on the glacier surface (≤0°C), and therefore can be ignored in statistics (Guo et al., 2022). We also noticed that the boundary of TP used in this study differs from that of some previous studies (e.g., Wang et al., 2020; Ma et al., 2021). The boundary we adopted is more reliable as it is based on geomorphology and formation processes that considers factors such as elevation, hydrological watershed, et., which is more completed and suitable for land surface process analysis (Zhang et al., 2013; Zhang et al., 2021).

Due to the heterogeneity of the climate and land surface, the dominant processes vary across the different sub-regions of the TP. For example, plant transpiration is expected to be the dominant process in the humid plant-soil systems which are more abundant in the eastern and southeastern TP, while soil evaporation is expected to be the dominant process in the middle to western TP where arid sparse-vegetated or bare soil cover is prevalent. The difference between these processes surely impacted both the ET magnitudes and the responses to the governing factors. In the eastern and southeastern TP where ET is higher due to the wet climate and high vegetation covers, there are strong correlations between Rn and ET indicating that biological cycles play an important role, and plant leaf stomatal openness and closure are closely related to the radiation force. In contrast, in the middle and western TP, we found high correlations between precipitation and ET in the middle and western TP due to the cold arid climate and sparse vegetation covers, and the abiotic processes are more dominant. Meanwhile, we should notice that these factors are not fully independent. Plants tend to grow more (high LAI) in regions where water is abundant, while higher LAI leads to higher Rn due to the generally low albedo of plant compared to soil. This may be more important in the energy-limited regions of southeastern TP.

4.3.2 Impact of cryosphere on surface water flux

Cryosphere element dynamics, such as glacier and snow, affect water flux processes significantly. The snow/ice sublimation constitutes as one of the most important aspects of water resources and hydrology in the higher altitude (MacDonald et al., 2010). Sublimation contributes significantly to the decrease in snow cover fraction during winter, especially in areas with thin snow cover, and more than half of the snow mass was lost by sublimation during winter in TP (Ueno et al., 2007; Qin et al., 2006). This study found that snow/ice sublimation (water phase change directly from solid to vapor) in TP is roughly 14mm/yr (median value of different product). It may lead to 4% of error if sublimation is not counted when estimating the total water flux released by TP to the atmosphere. The sublimation from snow and ice surfaces occurs primarily at high elevations when snow/ice covers large portions of the catchment and atmospheric conditions are cold and dry. The maximum sublimation

https://doi.org/10.5194/hess-2024-55
Preprint. Discussion started: 13 March 2024


Hydrology and Earth System Sciences Discussions

value is higher than 100mm/yr in TP (Figure 12). A recent observations study of Langtang Valley in the Central Himalaya in Nepal shows that the snow sublimation consumes more energy than evaporation, and the snow sublimation is 32~74 mm/yr during 2017~2019 (Stigter et al., 2021), which is consistent with the estimation by ETMonitor (48 mm/yr) (Zheng et al. 2022). Meanwhile, the melting of glaciers replenishes the downstream soil water and lead an increasing of water available, which will also enhance the ET process. A study has reported contrasting tendencies in ET between a wetland replenished by glaciers melting water and the nearby alpine steppe without the impact of glaciers in central TP (Ma et al., 2021).

5. Conclusion

To clarify the magnitude and variability of water vapour released to the atmosphere in TP, this study evaluated the performance of 22 ET products in Tibetan Plateau in terms of accuracy, spatial variation, temporal variation, ET components, response to environmental factors. The accuracy of ET products is validated by comparing with either ground flux tower observations or basin-scale water balance estimations. The spatiotemporal variations of ET and its components were intercompared, and the response of ET in TP to precipitation, net surface radiation and leaf area index was explored based on the Pearson correlation analysis. Following conclusions were obtained:

- According to our validation, the remote sensing high-resolution ET data from ETMonitor and PMLV2 generally showed comparable high accuracy as the regional MOD16STM ET product, with overall better accuracy than other global ET data with fine spatial resolution (~1km). The accuracy of these ET estimates was confirmed by the comparison with the water balance-based ET at basin scale, which further indicated overall accuracy of GLEAM and TerraClimate for the coarse-resolution ET products.
- The median and mean values of annual ET in the TP, according to the multiple products evaluated in this study, are 362.21 mm/yr and 350.34 mm/yr respectively, with a standard deviation of 42.46 mm/yr. Different products showed different spatial and temporal patterns, and large deviations occurred in the middle and western TP. Most products presented increasing trend of annual ET in TP from 2000 to 2020, and the rate varies depending on the products.
- The separate contributions of different components, i.e. plant transpiration, soil evaporation, interception loss, open water evaporation, and snow/ice sublimation, vary substantially even in cases in which total ET agrees well between different products, and soil evaporation accounts for most of ET. The contributions of open water evaporation and snow/ice sublimation are also not negligible.
- ET is regulated by precipitation, net radiation, and LAI. The effect of precipitation on ET is clearly illustrated, especially in the middle and northern TP. The net radiation plays significant role in the eastern TP, while a high correlation between ET and LAI was also found occasionally in the TP.

https://doi.org/10.5194/hess-2024-55
Preprint. Discussion started: 13 March 2024

Hydrology and Earth System Sciences
Discussions

Acknowledgements:

This work is funded by the Second Tibetan Plateau Scientific Expedition and Research Program (Grant no. 2019QZKK0206, 2019QZKK010308) and National Natural Science Foundation of China (Grant no. 42090014, 42171039). This work is also supported by the International Fellowship Initiative of CEOP – AEGIS and CSC Fellowship.

Author Contributions:

Dr. C. Zheng: Conceptualization, Methodology, Software, Validation, Formal analysis, Investigation, Resources, Data curation, Writing - original draft, Visualization. Prof. L. Jia: Conceptualization, Methodology, Resources, Data curation, Writing - review & editing, Supervision, Project administration, Funding acquisition. Dr. G Hu: Methodology, Validation, Writing - review & editing. Prof. M. Menenti: Writing - review & editing. Dr. J. Timmermans: Writing - review & editing.

Data availability:

The data in study are all from open accessed datasets. FLUXNET data is available from data portal of fluxnet (https://fluxnet.org/). The ChinaFLUX data is available from the data portal of National Ecosystem Research Network of China (http://www.cnern.org.cn/). TORP data and TPHiPr precipitation data is available from National Tibetan Plateau Data Center (http://data.tpdc.ac.cn/). GLASS datasets are available from the University of Maryland (http://glass.umd.edu/). MERRA2 and GLDAS data are available from the Goddard Earth Sciences Data and Information Services Center (https://disc.gsfc.nasa.gov/). The MODIS datasets are available from NASA Earthdata Search (https://search.earthdata.nasa.gov/). The ETMonitor ET is available from CASEARTH Data Sharing and Service Portal (https://data.casearth.cn/). The GLEAM product is available from its official site (www.gleam.eu). The MOD16-STM, EB ET, CR, PMLV2 and PMLV2-Tibet ET datasets are available from TPDC (https://data.tpdc.ac.cn/). The FLUXCOM ET dataset is available from its official website (www.fluxcom.org). The ERA5 and ERA5-Land datasets are available from the Copernicus Climate Data Store (https://cds.climate.copernicus.eu/). SSEBop is available from USGS (https://earlywarning.usgs.gov/ssebop/). TerraClimate is available from Climatology Lab (https://www.climatologylab.org/). SynthesisET is available from the Harvard Data public repository (https://doi.org/10.7910/DVN/ZGOUED). BESSv2 is available from the Seoul National University (https://www.environment.snu.ac.kr/bessv2).

Conflicts of Interest:

The authors declare that they have no conflict of interest.

https://doi.org/10.5194/hess-2024-55
Preprint. Discussion started: 13 March 2024


Hydrology and Earth System Sciences
Discussions

References

Abatzoglou, J. T., Dobrowski, S. Z., Parks, S. A., and Hegewisch, K. C.: TerraClimate, a high-resolution global dataset of monthly climate and climatic water balance from 1958-2015, Sci. Data, 5, https://doi.org/10.1038/sdata.2017.191, 2018.

Baldocchi, D. D.: How eddy covariance flux measurements have contributed to our understanding of Global Change Biology, https://doi.org/10.1111/gcb.14807, 2020.

Bibi, S., Wang, L., Li, X., Zhou, J., Chen, D., and Yao, T.: Climatic and associated cryospheric, biospheric, and hydrological changes on the Tibetan Plateau: a review, https://doi.org/10.1002/joc.5411, 2018.

Chang, Y., Qin, D., Ding, Y., Zhao, Q., and Zhang, S.: A modified MOD16 algorithm to estimate evapotranspiration over alpine meadow on the Tibetan Plateau, China, J. Hydrol., 561, 16–30, https://doi.org/10.1016/j.jhydrol.2018.03.054, 2018.

Chen, Y., Xia, J., Liang, S., Feng, J., Fisher, J. B., Li, X., Li, X., Liu, S., Ma, Z., Miyata, A., Mu, Q., Sun, L., Tang, J., Wang, K., Wen, J., Xue, Y., Yu, G., Zha, T., Zhang, L., Zhang, Q., Zhao, T., Zhao, L., and Yuan, W.: Comparison of satellite-based evapotranspiration models over terrestrial ecosystems in China, Remote Sens. Environ., 140, 279–293, https://doi.org/10.1016/j.rse.2013.08.045, 2014.

Chen, D., Xu, B., Yao, T., Guo, Z., Cui, P., Chen, F., Zhang, R., Zhang, X., Zhang, Y., Fan, J., Hou, Z., and Zhang, T.: Assessment of past, present and future environmental changes on the Tibetan Plateau, Chinese Sci. Bull., 60, https://doi.org/10.1360/N972014-01370, 2015.

Chen, J., Tan, H., Ji, Y., Tang, Q., Yan, L., Chen, Q., and Tan, D.: Evapotranspiration components dynamic of highland barley using PML ET product in Tibet, Remote Sens., 13, https://doi.org/10.3390/rs13234884, 2021.

Chen, J. M. and Liu, J.: Evolution of evapotranspiration models using thermal and shortwave remote sensing data, Remote Sens. Environ., 237, 111594, https://doi.org/10.1016/j.rse.2019.111594, 2020.

Chen, Q., Jia, L., Menenti, M., Hutjes, R., Hu, G., Zheng, C., and Wang, K.: A numerical analysis of aggregation error in evapotranspiration estimates due to heterogeneity of soil moisture and leaf area index, Agric. For. Meteorol., 269–270, 335–350, https://doi.org/10.1016/j.agrformet.2019.02.017, 2019.

Chen, X., Su, Z., Ma, Y., Trigo, I., and Gentine, P.: Remote Sensing of Global Daily Evapotranspiration based on a Surface Energy Balance Method and Reanalysis Data, J. Geophys. Res. Atmos., 126, 1–22, https://doi.org/10.1029/2020JD032873, 2021.

Crago, R. D., Szilagyi, J., and Qualls, R.: Comment on: “a review of the complementary principle of evaporation: From the original linear relationship to generalized nonlinear functions” by Han and Tian (2020), Hydrol. Earth Syst. Sci., 25, https://doi.org/10.5194/hess-25-63-2021, 2021.

Cui, J., Tian, L., Wei, Z., Huntingford, C., Wang, P., Cai, Z., Ma, N., and Wang, L.: Quantifying the Controls on Evapotranspiration Partitioning in the Highest Alpine Meadow Ecosystem, Water Resour. Res., 56, https://doi.org/10.1029/2019WR024815, 2020.

Elnashar, A., Wang, L., Wu, B., Zhu, W., and Zeng, H.: Synthesis of global actual evapotranspiration from 1982 to 2019,

Earth Syst. Sci. Data, 13, 447–480, https://doi.org/10.5194/essd-13-447-2021, 2021.

Foken, T.: The energy balance closure problem: An overview, Ecol. Appl., 18, https://doi.org/10.1890/06-0922.1, 2008.

Gelaro, R., McCarty, W., Suárez, M. J., Todling, R., Molod, A., Takacs, L., Randles, C. A., Darmenov, A., Bosilovich, M. G., Reichle, R., Wargan, K., Coy, L., Cullather, R., Draper, C., Akella, S., Buchard, V., Conaty, A., da Silva, A. M., Gu, W., Kim, G. K., Koster, R., Lucchesi, R., Merkova, D., Nielsen, J. E., Partyka, G., Pawson, S., Putman, W., Rienecker, M., Schubert, S. D., Sienkiewicz, M., and Zhao, B.: The modern-era retrospective analysis for research and applications, version 2 (MERRA-2), J. Clim., 30, https://doi.org/10.1175/JCLI-D-16-0758.1, 2017.

Gupta, H. V., Kling, H., Yilmaz, K. K., and Martinez, G. F.: Decomposition of the mean squared error and NSE performance criteria: Implications for improving hydrological modelling, J. Hydrol., 377, https://doi.org/10.1016/j.jhydrol.2009.08.003, 2009.

Han, S. and Tian, F.: A review of the complementary principle of evaporation: From the original linear relationship to generalized nonlinear functions, https://doi.org/10.5194/hess-24-2269-2020, 2020.

He, J., Yang, K., Tang, W., Lu, H., Qin, J., Chen, Y., and Li, X.: The first high-resolution meteorological forcing dataset for land process studies over China, Sci. Data, 7, https://doi.org/10.1038/s41597-020-0369-y, 2020.

Hersbach, H., Bell, B., Berrisford, P., Hirahara, S., Horányi, A., Muñoz-Sabater, J., Nicolas, J., Peubey, C., Radu, R., Schepers, D., Simmons, A., Soci, C., Abdalla, S., Abellan, X., Balsamo, G., Bechtold, P., Biavati, G., Bidlot, J., Bonavita, M., De Chiara, G., Dahlgren, P., Dee, D., Diamantakis, M., Dragani, R., Flemming, J., Forbes, R., Fuentes, M., Geer, A., Haimberger, L., Healy, S., Hogan, R. J., Hólm, E., Janisková, M., Keeley, S., Laloyaux, P., Lopez, P., Lupu, C., Radnoti, G., de Rosnay, P., Rozum, I., Vamborg, F., Villaume, S., and Thépaut, J. N.: The ERA5 global reanalysis, Q. J. R. Meteorol. Soc., 146, https://doi.org/10.1002/qj.3803, 2020.

Hu, Z., Yu, G., Zhou, Y., Sun, X., Li, Y., Shi, P., Wang, Y., Song, X., Zheng, Z., Zhang, L., and Li, S.: Partitioning of evapotranspiration and its controls in four grassland ecosystems: Application of a two-source model, Agric. For. Meteorol., 149, https://doi.org/10.1016/j.agrformet.2009.03.014, 2009.

Immerzeel, W. W., Lutz, A. F., Andrade, M., Bahl, A., Biemans, H., Bolch, T., Hyde, S., Brumby, S., Davies, B. J., Elmore, A. C., Emmer, A., Feng, M., Fernández, A., Haritashya, U., Kargel, J. S., Koppes, M., Kraaijenbrink, P. D. A., Kulkarni, A. V., Mayewski, P. A., Nepal, S., Pacheco, P., Painter, T. H., Pellicciotti, F., Rajaram, H., Rupper, S., Sinisalo, A., Shrestha, A. B., Viviroli, D., Wada, Y., Xiao, C., Yao, T., and Baillie, J. E. M.: Importance and vulnerability of the world's water towers, Nature, 577, https://doi.org/10.1038/s41586-019-1822-y, 2020.

Jia L., Zheng C., Hu G.C., Menenti M.: 4.03 - Evapotranspiration, In Comprehensive Remote Sensing, edited by Shunlin Liang, Elsevier, Oxford. http://10.1016/B978-0-12-409548-9.10353-7, 2018.

Jia, A., Jiang, B., Liang, S., Zhang, X., and Ma, H.: Validation and spatiotemporal analysis of CERES surface net radiation product, Remote Sens., 8, https://doi.org/10.3390/rs8020090, 2016.

Jiang, Y., Yang, K., Qi, Y., Zhou, X., He, J., Lu, H., Li, X., Chen, Y., Li, X., Zhou, B., Mamtimin, A., Shao, C., Ma, X., Tian, J., and Zhou, J.: TPHiPr: a long-term (1979-2020) high-accuracy precipitation dataset (1/30°daily) for the Third Pole region

based on high-resolution atmospheric modeling and dense observations, Earth Syst. Sci. Data, 15, https://doi.org/10.5194/essd-15-621-2023, 2023.

Jiang, Y., Tang, R., and Li, Z. L.: A physical full-factorial scheme for gap-filling of eddy covariance measurements of daytime evapotranspiration, Agric. For. Meteorol., 323, https://doi.org/10.1016/j.agrformet.2022.109087, 2022.

Jiao, D., Xu, N., Yang, F., and Xu, K.: Evaluation of spatial-temporal variation performance of ERA5 precipitation data in China, Sci. Rep., 11, https://doi.org/10.1038/s41598-021-97432-y, 2021.

Jung, M., Koirala, S., Weber, U., Ichii, K., Gans, F., Camps-Valls, G., Papale, D., Schwalm, C., Tramontana, G., and Reichstein, M.: The FLUXCOM ensemble of global land-atmosphere energy fluxes, Sci. Data, 6, 1–14, https://doi.org/10.1038/s41597-019-0076-8, 2019.

Kato, T., Tang, Y., Gu, S., Hirota, M., Cui, X., Du, M., Li, Y., Zhao, X., and Oikawa, T.: Seasonal patterns of gross primary production and ecosystem respiration in an alpine meadow ecosystem on the Qinghai-Tibetan Plateau, J. Geophys. Res. D Atmos., 109, https://doi.org/10.1029/2003JD003951, 2004.

Khan, M. S., Baik, J., and Choi, M.: Inter-comparison of evapotranspiration datasets over heterogeneous landscapes across Australia, Adv. Sp. Res., 66, https://doi.org/10.1016/j.asr.2020.04.037, 2020.

Kuang, X. and Jiao, J. J.: Review on climate change on the Tibetan plateau during the last half century, https://doi.org/10.1002/2015JD024728, 2016.

Li, B., Rodell, M., Kumar, S., Beaudoing, H. K., Getirana, A., Zaitchik, B. F., de Goncalves, L. G., Cossetin, C., Bhanja, S., Mukherjee, A., Tian, S., Tangdamrongsub, N., Long, D., Nanteza, J., Lee, J., Policelli, F., Goni, I. B., Daira, D., Bila, M., de Lannoy, G., Mocko, D., Steele-Dunne, S. C., Save, H., and Bettadpur, S.: Global GRACE Data Assimilation for Groundwater and Drought Monitoring: Advances and Challenges, Water Resour. Res., 55, https://doi.org/10.1029/2018WR024618, 2019.

Li, X., Long, D., Han, Z., Scanlon, B. R., Sun, Z., Han, P., and Hou, A.: Evapotranspiration Estimation for Tibetan Plateau Headwaters Using Conjoint Terrestrial and Atmospheric Water Balances and Multisource Remote Sensing, Water Resour. Res., 55, https://doi.org/10.1029/2019WR025196, 2019.

Li, Z., Feng, Q., Li, Z., Yuan, R., Gui, J., and Lv, Y.: Climate background, fact and hydrological effect of multiphase water transformation in cold regions of the Western China: A review, https://doi.org/10.1016/j.earscirev.2018.12.004, 2019.

Li, B., Ryu, Y., Jiang, C., Dechant, B., Liu, J., Yan, Y., and Li, X.: BESSv2.0: A satellite-based and coupled-process model for quantifying long-term global land–atmosphere fluxes, Remote Sens. Environ., 295, https://doi.org/10.1016/j.rse.2023.113696, 2023.

Li, X., Li, X., Li, Z., Ma, M., Wang, J., Xiao, Q., Liu, Q., Che, T., Chen, E., Yan, G., Hu, Z., Zhang, L., Chu, R., Su, P., Liu, Q., Liu, S., Wang, J., Niu, Z., Chen, Y., Jin, R., Wang, W., Ran, Y., Xin, X., and Ren, H.: Watershed allied telemetry experimental research, J. Geophys. Res. Atmos., 114, https://doi.org/10.1029/2008JD011590, 2009.

Liu, S., Li, X., Xu, Z., Che, T., Xiao, Q., Ma, M., Liu, Q., Jin, R., Guo, J., Wang, L., Wang, W., Qi, Y., Li, H., Xu, T., Ran, Y., Hu, X., Shi, S., Zhu, Z., Tan, J., Zhang, Y., and Ren, Z.: The Heihe Integrated Observatory Network: A Basin-Scale Land Surface Processes Observatory in China, Vadose Zo. J., 17, https://doi.org/10.2136/vzj2018.04.0072, 2018.

https://doi.org/10.5194/hess-2024-55
Preprint. Discussion started: 13 March 2024

Ma, N., Zhang, Y., Guo, Y., Gao, H., Zhang, H., and Wang, Y.: Environmental and biophysical controls on the evapotranspiration over the highest alpine steppe, J. Hydrol., 529, https://doi.org/10.1016/j.jhydrol.2015.09.013, 2015.

Ma, N., Szilagyi, J., and Zhang, Y.: Calibration-Free Complementary Relationship Estimates Terrestrial Evapotranspiration Globally, Water Resour. Res., 57, 1–27, https://doi.org/10.1029/2021WR029691, 2021.

Ma, N. and Zhang, Y.: Increasing Tibetan Plateau terrestrial evapotranspiration primarily driven by precipitation, Agric. For. Meteorol., 317, https://doi.org/10.1016/j.agrformet.2022.108887, 2022.

Ma, Y., Hu, Z., Xie, Z., Ma, W., Wang, B., Chen, X., Li, M., Zhong, L., Sun, F., Gu, L., Han, C., Zhang, L., Liu, X., Ding, Z., Sun, G., Wang, S., Wang, Y., and Wang, Z.: A long-term (2005–2016) dataset of hourly integrated land–atmosphere interaction observations on the Tibetan Plateau, Earth Syst. Sci. Data, 12, https://doi.org/10.5194/essd-12-2937-2020, 2020.

Ma, Y., Kang, S., Zhu, L., Xu, B., Tian, L., and Yao, T.: Roof of the World: Tibetan observation and research platform, Bull. Am. Meteorol. Soc., 89, https://doi.org/10.1175/2008BAMS2545.1, 2008.

Martens, B., Miralles, D. G., Lievens, H., Van Der Schalie, R., De Jeu, R. A. M., Fernández-Prieto, D., Beck, H. E., Dorigo, W. A., and Verhoest, N. E. C.: GLEAM v3: Satellite-based land evaporation and root-zone soil moisture, Geosci. Model Dev., 10, 1903–1925, https://doi.org/10.5194/gmd-10-1903-2017, 2017.

Miralles, D. G., Holmes, T. R. H., De Jeu, R. A. M., Gash, J. H., Meesters, A. G. C. A., and Dolman, A. J.: Global land-surface evaporation estimated from satellite-based observations, Hydrol. Earth Syst. Sci., 15, 453–469, https://doi.org/10.5194/hess-15-453-2011, 2011.

Miralles, D. G., Brutsaert, W., Dolman, A. J., and Gash, J. H.: On the Use of the Term "Evapotranspiration," https://doi.org/10.1029/2020WR028055, 2020.

Morton, F. I.: Operational estimates of areal evapotranspiration and their significance to the science and practice of hydrology, J. Hydrol., 66, https://doi.org/10.1016/0022-1694(83)90177-4, 1983.

Mu, Q., Heinsch, F. A., Zhao, M., and Running, S. W.: Mu, Q., Zhao, M., and Running, S. W.: Improvements to a MODIS global terrestrial evapotranspiration algorithm, Remote Sens. Environ., 111, https://doi.org/10.1016/j.rse.2007.04.015, 2007.

Mu, Q., Zhao, M., and Running, S. W.: Improvements to a MODIS global terrestrial evapotranspiration algorithm, Remote Sens. Environ., 115, https://doi.org/10.1016/j.rse.2011.02.019, 2011.

Mueller, B., Hirschi, M., Jimenez, C., Ciais, P., Dirmeyer, P. A., Dolman, A. J., Fisher, J. B., Jung, M., Ludwig, F., Maignan, F., Miralles, D. G., McCabe, M. F., Reichstein, M., Sheffield, J., Wang, K., Wood, E. F., Zhang, Y., and Seneviratne, S. I.: Benchmark products for land evapotranspiration: LandFlux-EVAL multi-data set synthesis, Hydrol. Earth Syst. Sci., 17, 3707–3720, https://doi.org/10.5194/hess-17-3707-2013, 2013.

Muñoz-Sabater, J., Dutra, E., Agustí-Panareda, A., Albergel, C., Arduini, G., Balsamo, G., Boussetta, S., Choulga, M., Harrigan, S., Hersbach, H., Martens, B., Miralles, D. G., Piles, M., Rodríguez-Fernández, N. J., Zsoter, E., Buontempo, C., and Thépaut, J. N.: ERA5-Land: A state-of-the-art global reanalysis dataset for land applications, Earth Syst. Sci. Data, 13, https://doi.org/10.5194/essd-13-4349-2021, 2021.

Rodell, M., Houser, P. R., Jambor, U., Gottschalck, J., Mitchell, K., Meng, C. J., Arsenault, K., Cosgrove, B., Radakovich, J.,

https://doi.org/10.5194/hess-2024-55
Preprint. Discussion started: 13 March 2024


Hydrology and Earth System Sciences
Discussions

Bosilovich, M., Entin, J. K., Walker, J. P., Lohmann, D., and Toll, D.: The Global Land Data Assimilation System, Bull. Am. Meteorol. Soc., 85, https://doi.org/10.1175/BAMS-85-3-381, 2004.

Senay, G. B., Kagone, S., and Velpuri, N. M.: Operational global actual evapotranspiration: Development, evaluation, and dissemination, Sensors (Switzerland), 20, https://doi.org/10.3390/s20071915, 2020.

Shang, L., Zhang, Y., Lü, S., and Wang, S.: Energy exchange of an alpine grassland on the eastern Qinghai-Tibetan Plateau, Sci. Bull., 60, https://doi.org/10.1007/s11434-014-0685-8, 2015.

Shang, K., Yao, Y., Di, Z., Jia, K., Zhang, X., Fisher, J. B., Chen, J., Guo, X., Yang, J., Yu, R., Xie, Z., Liu, L., Ning, J., & Zhang, L.: Coupling physical constraints with machine learning for satellite-derived evapotranspiration of the Tibetan Plateau. Remote Sensing of Environment, 289. https://doi.org/10.1016/j.rse.2023.113519, 2023.

Shen, M., Piao, S., Jeong, S. J., Zhou, L., Zeng, Z., Ciais, P., Chen, D., Huang, M., Jin, C. S., Li, L. Z. X., Li, Y., Myneni, R. B., Yang, K., Zhang, G., Zhang, Y., and Yao, T.: Evaporative cooling over the Tibetan Plateau induced by vegetation growth, Proc. Natl. Acad. Sci. U. S. A., 112, https://doi.org/10.1073/pnas.1504418112, 2015.

Song, L., Zhuang, Q., Yin, Y., Zhu, X., and Wu, S.: Spatio-temporal dynamics of evapotranspiration on the Tibetan Plateau from 2000 to 2010, Environ. Res. Lett., 12, https://doi.org/10.1088/1748-9326/aa527d, 2017.

Stigter, E. E., Steiner, J. F., Koch, I., Saloranta, T. M., Kirkham, J. D., and Immerzeel, W. W.: Energy and mass balance dynamics of the seasonal snowpack at two high-altitude sites in the Himalaya, Cold Reg. Sci. Technol., 183, https://doi.org/10.1016/j.coldregions.2021.103233, 2021.

Sun, H., Su, F., Yao, T., He, Z., Tang, G., Huang, J., Zheng, B., Meng, F., Ou, T., and Chen, D.: General overestimation of ERA5 precipitation in flow simulations for High Mountain Asia basins, Environ. Res. Commun., 3, https://doi.org/10.1088/2515-7620/ac40f0, 2021.

Sun, J., Yang, K., Yu, Y., Lu, H., and Lin, Y.: Land–Atmosphere Interactions Partially Offset the Accelerated Tibetan Plateau Water Cycle through Dynamical Processes, J. Clim., 36, https://doi.org/10.1175/JCLI-D-22-0686.1, 2023.

Twine, T. E., Kustas, W. P., Norman, J. M., Cook, D. R., Houser, P. R., Meyers, T. P., Prueger, J. H., Starks, P. J., and Wesely, M. L.: Correcting eddy-covariance flux underestimates over a grassland, Agric. For. Meteorol., 103, https://doi.org/10.1016/S0168-1923(00)00123-4, 2000.

Ueno, K., Tanaka, K., Tsutsui, H., and Li, M.: Snow cover conditions in the Tibetan Plateau observed during the winter of 2003/2004, in: Arctic, Antarctic, and Alpine Research, https://doi.org/10.1657/1523-0430(2007)39[152:SCCITT]2.0.CO;2, 2007.

Wang, L., Han, S., Tian, F., Li, K., Li, Y., Tudaji, M., Cao, X., Nan, Y., Cui, T., Zheng, X., Hu, Z., Wang, W., and Yang, Y. Z.: The Evaporation on the Tibetan Plateau Stops Increasing in the Recent Two Decades, J. Geophys. Res. Atmos., 127, https://doi.org/10.1029/2022JD037377, 2022.

Wang, W., Li, J., Yu, Z., Ding, Y., Xing, W., and Lu, W.: Satellite retrieval of actual evapotranspiration in the Tibetan Plateau: Components partitioning, multidecadal trends and dominated factors identifying, J. Hydrol., 559, https://doi.org/10.1016/j.jhydrol.2018.02.065, 2018.

Wang, Z., Wu, R., and Huang, G.: Low-frequency snow changes over the Tibetan Plateau, Int. J. Climatol., 38, https://doi.org/10.1002/joc.5221, 2018.

Wei, Y., Lu, H., Wang, J., Wang, X., and Sun, J.: Dual Influence of Climate Change and Anthropogenic Activities on the Spatiotemporal Vegetation Dynamics Over the Qinghai-Tibetan Plateau From 1981 to 2015, Earth's Futur., 10, https://doi.org/10.1029/2021EF002566, 2022.

Wu, G. X., Zhuo, H. F., Wang, Z. Q., and Liu, Y. M.: Two types of summertime heating over the Asian large-scale orography and excitation of potential-vorticity forcing I. Over Tibetan Plateau, Sci. China Earth Sci., 59, https://doi.org/10.1007/s11430-016-5328-2, 2016.

Xiao, Z., Liang, S., Wang, J., Chen, P., Yin, X., Zhang, L., and Song, J.: Use of general regression neural networks for generating the GLASS leaf area index product from time-series MODIS surface reflectance, IEEE Trans. Geosci. Remote Sens., 52, https://doi.org/10.1109/TGRS.2013.2237780, 2014.

Xiao, Z., Song, J., Yang, H., Sun, R., and Li, J.: A 250 m resolution global leaf area index product derived from MODIS surface reflectance data, Int. J. Remote Sens., 43, https://doi.org/10.1080/01431161.2022.2039415, 2022.

Xie, W., Yi, S., Leng, C., Xia, D., Li, M., Zhong, Z., and Ye, J.: The evaluation of IMERG and ERA5-Land daily precipitation over China with considering the influence of gauge data bias, Sci. Rep., 12, https://doi.org/10.1038/s41598-022-12307-0, 2022.

Xue, B. L., Wang, L., Li, X., Yang, K., Chen, D., and Sun, L.: Evaluation of evapotranspiration estimates for two river basins on the Tibetan Plateau by a water balance method, J. Hydrol., 492, 290–297, https://doi.org/10.1016/j.jhydrol.2013.04.005, 2013.

Yang, C., Liu, H., Li, Q., Wang, X., Ma, W., Liu, C., Fang, X., Tang, Y., Shi, T., Wang, Q., Xu, Y., Zhang, J., Li, X., Xu, G., Chen, J., Su, M., Wang, S., Wu, J., Huang, L., Li, X., and Wu, G.: Human expansion into Asian highlands in the 21st Century and its effects, Nat. Commun., 13, https://doi.org/10.1038/s41467-022-32648-8, 2022.

Yang, K., Wu, H., Qin, J., Lin, C., Tang, W., and Chen, Y.: Recent climate changes over the Tibetan Plateau and their impacts on energy and water cycle: A review, Glob. Planet. Change, 112, https://doi.org/10.1016/j.gloplacha.2013.12.001, 2014.

Yang, W., Wang, Y., Liu, X., Zhao, H., Shao, R., and Wang, G.: Evaluation of the rescaled complementary principle in the estimation of evaporation on the Tibetan Plateau, Sci. Total Environ., 699, https://doi.org/10.1016/j.scitotenv.2019.134367, 2020.

Yang, Y., Chen, R., Song, Y., Han, C., Liu, Z., and Liu, J.: Evaluation of five complementary relationship models for estimating actual evapotranspiration during soil freeze-thaw cycles, Hydrol. Res., 52, https://doi.org/10.2166/nh.2021.093, 2021.

Yang, Y., Roderick, M. L., Guo, H., Miralles, D. G., Zhang, L., Fatichi, S., Luo, X., Zhang, Y., McVicar, T. R., Tu, Z., Keenan, T. F., Fisher, J. B., Gan, R., Zhang, X., Piao, S., Zhang, B., and Yang, D.: Evapotranspiration on a greening Earth, https://doi.org/10.1038/s43017-023-00464-3, 2023.

Yao, T., Thompson, L., Yang, W., Yu, W., Gao, Y., Guo, X., Yang, X., Duan, K., Zhao, H., Xu, B., Pu, J., Lu, A., Xiang, Y., Kattel, D. B., and Joswiak, D.: Different glacier status with atmospheric circulations in Tibetan Plateau and surroundings, Nat. Clim. Chang., 2, https://doi.org/10.1038/nclimate1580, 2012.

https://doi.org/10.5194/hess-2024-55
Preprint. Discussion started: 13 March 2024

Yao, T., Xue, Y., Chen, D., Chen, F., Thompson, L., Cui, P., Koike, T., Lau, W. K. M., Lettenmaier, D., Mosbrugger, V., Zhang, R., Xu, B., Dozier, J., Gillespie, T., Gu, Y., Kang, S., Piao, S., Sugimoto, S., Ueno, K., Wang, L., Wang, W., Zhang, F., Sheng, Y., Guo, W., Ailikun, Yang, X. X., Ma, Y., Shen, S. S. P., Su, Z., Chen, F., Liang, S., Liu, Y., Singh, V. P., Yang, K., Yang, D., Zhao, X., Qian, Y., Zhang, Y., and Li, Q.: Recent third pole's rapid warming accompanies cryospheric melt and water cycle intensification and interactions between monsoon and environment: Multidisciplinary approach with observations, modeling, and analysis, Bull. Am. Meteorol. Soc., 100, https://doi.org/10.1175/BAMS-D-17-0057.1, 2019.

Yao, Y., Liang, S., Li, X., Hong, Y., Fisher, J. B., Zhang, N., Chen, J., Cheng, J., Zhao, S., Zhang, X., Jiang, B., Sun, L., Jia, K., Wang, K., Chen, Y., Mu, Q., and Feng, F.: Bayesian multimodel estimation of global terrestrial latent heat flux from eddy covariance, meteorological, and satellite observations, J. Geophys. Res., 119, https://doi.org/10.1002/2013JD020864, 2014.

Yu, G. R., Wen, X. F., Sun, X. M., Tanner, B. D., Lee, X., and Chen, J. Y.: Overview of ChinaFLUX and evaluation of its eddy covariance measurement, Agric. For. Meteorol., 137, https://doi.org/10.1016/j.agrformet.2006.02.011, 2006.

Yuan, L., Ma, Y., Chen, X., Wang, Y., and Li, Z.: An Enhanced MOD16 Evapotranspiration Model for the Tibetan Plateau During the Unfrozen Season, J. Geophys. Res. Atmos., 126, https://doi.org/10.1029/2020JD032787, 2021.

Zhang, G., Yao, T., Xie, H., Kang, S., and Lei, Y.: Increased mass over the Tibetan Plateau: From lakes or glaciers?, Geophys. Res. Lett., 40, https://doi.org/10.1002/grl.50462, 2013.

Zhang, K., Kimball, J. S., Nemani, R. R., and Running, S. W.: A continuous satellite-derived global record of land surface evapotranspiration from 1983 to 2006, Water Resour. Res., 46, https://doi.org/10.1029/2009WR008800, 2010.

Zhang, T., Gebremichael, M., Meng, X., Wen, J., Iqbal, M., Jia, D., et al. Climate-related trends of actual evapotranspiration over the Tibetan Plateau (1961–2010). International Journal of Climatology, 38(S1), e48–e56. https://doi.org/10.1002/joc.5350, 2018.

Zhang, Y., Kong, D., Gan, R., Chiew, F. H. S., McVicar, T. R., Zhang, Q., and Yang, Y.: Coupled estimation of 500 m and 8-day resolution global evapotranspiration and gross primary production in 2002–2017, Remote Sens. Environ., 222, 165–182, https://doi.org/10.1016/j.rse.2018.12.031, 2019.

Zhang. Y., Li B., Liu L., Zheng D: Redetermine the region and boundaries of Tibetan Plateau, Geogr. Res., 40, https://doi.org/10.11821/dlyj020210138, 2021.

Zheng, C., Jia, L., and Hu, G.: Global land surface evapotranspiration monitoring by ETMonitor model driven by multi-source satellite earth observations, J. Hydrol., 613, 128444, https://doi.org/10.1016/j.jhydrol.2022.128444, 2022.

Zheng, C., Jia, L., Hu, G., Lu, J., Wang, K., and Li, Z.: Global Evapotranspiration Derived by ETMonitor Model based on Earth Observations, in: International Geoscience and Remote Sensing Symposium (IGARSS), 222–225, 2016.

Zhu, W., Wang, Y., and Jia, S.: A remote sensing-based method for daily evapotranspiration mapping and partitioning in a poorly gauged basin with arid ecosystems in the Qinghai-Tibet Plateau, J. Hydrol., 616, https://doi.org/10.1016/j.jhydrol.2022.128807, 2023.